NUREG/IA-0414

International Agreement Report

Comparison of the U.S. NRC PARCS Core Neutronics Simulator Against In-Core Detector Measurements for LWR Applications

Prepared by:
C. Demaziére, M. Stálek, P. Vinal

Division of Nuclear Engineering
Chalmers University of Technology
SE-41296 Gothenburg
Sweden

A. Calvo, NRC Project Manager

Office of Nuclear Regulatory Research
U.S. Nuclear Regulatory Commission
Washington, DC 20555-0001

Manuscript Completed: February 2011
Date Published: April 2012

Prepared as part of
The Agreement on Research Participation and Technical Exchange
Under the Thermal-Hydraulic Code Applications and Maintenance Program (CAMP)

Published by
U.S. Nuclear Regulatory Commission

AVAILABILITY OF REFERENCE MATERIALS IN NRC PUBLICATIONS

NRC Reference Material

As of November 1999, you may electronically access NUREG-series publications and other NRC records at NRC's Public Electronic Reading Room at http://www.nrc.gov/reading-rm.html. Publicly released records include, to name a few, NUREG-series publications; *Federal Register* notices; applicant, licensee, and vendor documents and correspondence; NRC correspondence and internal memoranda; bulletins and information notices; inspection and investigative reports; licensee event reports; and Commission papers and their attachments.

NRC publications in the NUREG series, NRC regulations, and *Title 10, Energy*, in the Code of *Federal Regulations* may also be purchased from one of these two sources.

1. The Superintendent of Documents
   U.S. Government Printing Office
   Mail Stop SSOP
   Washington, DC 20402–0001
   Internet: bookstore.gpo.gov
   Telephone: 202-512-1800
   Fax: 202-512-2250
2. The National Technical Information Service
   Springfield, VA 22161–0002
   www.ntis.gov
   1–800–553–6847 or, locally, 703–605–6000

A single copy of each NRC draft report for comment is available free, to the extent of supply, upon written request as follows:

Address: U.S. Nuclear Regulatory Commission
Office of Administration
Publications Branch
Washington, DC 20555-0001
E-mail: DISTRIBUTION.RESOURCE@NRC.GOV
Facsimile: 301–415–2289

Some publications in the NUREG series that are posted at NRC's Web site address http://www.nrc.gov/reading-rm/doc-collections/nuregs are updated periodically and may differ from the last printed version. Although references to material found on a Web site bear the date the material was accessed, the material available on the date cited may subsequently be removed from the site.

Non-NRC Reference Material

Documents available from public and special technical libraries include all open literature items, such as books, journal articles, and transactions, *Federal Register* notices, Federal and State legislation, and congressional reports. Such documents as theses, dissertations, foreign reports and translations, and non-NRC conference proceedings may be purchased from their sponsoring organization.

Copies of industry codes and standards used in a substantive manner in the NRC regulatory process are maintained at—

The NRC Technical Library
Two White Flint North
11545 Rockville Pike
Rockville, MD 20852–2738

These standards are available in the library for reference use by the public. Codes and standards are usually copyrighted and may be purchased from the originating organization or, if they are American National Standards, from—

American National Standards Institute
11 West 42nd Street
New York, NY 10036–8002
www.ansi.org
212–642–4900

Legally binding regulatory requirements are stated only in laws; NRC regulations; licenses, including technical specifications; or orders, not in NUREG-series publications. The views expressed in contractor-prepared publications in this series are not necessarily those of the NRC.

The NUREG series comprises (1) technical and administrative reports and books prepared by the staff (NUREG–XXXX) or agency contractors (NUREG/CR–XXXX), (2) proceedings of conferences (NUREG/CP–XXXX), (3) reports resulting from international agreements (NUREG/IA–XXXX), (4) brochures (NUREG/BR–XXXX), and (5) compilations of legal decisions and orders of the Commission and Atomic and Safety Licensing Boards and of Directors' decisions under Section 2.206 of NRC's regulations (NUREG–0750).

NUREG/IA-0414

International Agreement Report

Comparison of the U.S. NRC PARCS Core Neutronics Simulator Against In-Core Detector Measurements for LWR Applications

Prepared by:
C. Demaziére, M. Stálek, P. Vinal

Division of Nuclear Engineering
Chalmers University of Technology
SE-41296 Gothenburg
Sweden

A. Calvo, NRC Project Manager

Office of Nuclear Regulatory Research
U.S. Nuclear Regulatory Commission
Washington, DC 20555-0001

Manuscript Completed: February 2011
Date Published: April 2012

Prepared as part of
The Agreement on Research Participation and Technical Exchange
Under the Thermal-Hydraulic Code Applications and Maintenance Program (CAMP)

Published by
U.S. Nuclear Regulatory Commission

TABLE OF CONTENTS

LIST OF FIGURES

LIST OF TABLES

Page

ACKNOWLEDGMENT

The authors wish to thank Prof. Tom Downar, Dr. Yunlin Xu, and Dr. Tomasz Kozlowski for their help with the PARCS code and the PMAXS files, as well as their feedback about this work.

Ringhals AB, Forsmark Kraftgrupp AB and Vattenfall Nuclear Fuel AB are acknowledged for providing the plant data. In particular, the authors wish to thank Urban Sandberg, Mattias Carlsson and Gustav Andhill from Ringhals AB; Dr. Jyrki Peltonen and Dr. Gustav Dominicus from Forsmark Kraftgrupp AB; Dr. Hongwu Cheng from Vattenfall Nuclear Fuel AB.

The Swedish Radiation Safety Authority (SSM) is acknowledged for the financial support.

ABBREVIATIONS

ANM	Analytic nodal method
BWR	Boiling water reactor
LWR	Light water reactor
MIC	Movable in-core
NEM	Nodal expansion method
NPP	Nuclear power plant
PARCS	Purdue Advanced Reactor Core Simulator
PMAXS	Purdue macroscopic cross-section
PWR	Pressurized water reactor
RPF	Relative power fraction
Sm-149	Samarium-149
SSM	The Swedish Radiation Safety Authority
TIP	Traversing incore prove
U.S. NRC	The United States Nuclear Regulatory Commission
Xe-135	Xenon-135

EXECUTIVE SUMMARY

The safety analysis of a Nuclear Power Plant (NPP) is based on the application of complex computer codes that are able to simulate the physical behaviour of the system under normal operations and abnormal conditions. Therefore, such codes must be extensively and continuously verified and validated in order to demonstrate their reliability.

In this context, the current report presents an assessment study for the U.S. NRC 3-D neutronic core simulator PARCS, and it includes an evaluation of the performances of the code for LWRs applications. For this purpose, the cores of the Swedish Ringhals-3 Pressurized Water Reactor (PWR) unit and the Forsmark-2 Boiling Water Reactor (BWR) unit were modeled with PARCS. As regards the cross-sections needed for this kind of calculations, they were prepared by following a special procedure developed by the present authors since core material data were only available in the format of library and restart files created by the SIMULATE-3 neutronic core simulator. Correspondingly, a new cross-section interface was developed and verified by the Division of Nuclear Engineering, Chalmers University of Technology, in order to convert the SIMULATE-3 data into data suitable for PARCS. Thereafter, the PARCS models developed for Ringhals-3 and Forsmark-2 were used for neutronic core analyses, at different operating conditions, along several fuel cycles. The results achieved from these simulations were then compared against the axial power and the radial power distribution estimated from the measurements that were provided by the owners of the plants.

In the PWR case, the PARCS simulations predict satisfactorily both the core axial power profile and the core radial power distribution, although, in some cases, the deviations between calculated and measured data exhibit trends that need further investigations. For instance, the PARCS simulation at the beginning of a fuel cycle seems to overestimate the power in the center of the core and to underestimate the power at the periphery, whereas, at the end of a fuel cycle, the situation is opposite.

In the BWR case, the core axial profile was predicted in a reasonable manner, but quite significant discrepancies for the radial power distribution was found. The current work suggests that such a disagreement might be due to the inability of PARCS to properly model multiple composition control rods. In fact the largest deviations in the computed power from the measurements were observed for those fuel assemblies placed in the neighborhood of control rods.

1. INTRODUCTION

The safety analysis of a Nuclear Power Plant (NPP) is based on the application of complex computer codes that are able to simulate the physical behaviour of the system under normal operations and abnormal conditions. Therefore, an extensive verification and validation work of these computational tools is crucial, so that safety analyses based on such tools can be considered as reliable.

The division of Nuclear Engineering at Chalmers University of Technology has been active in the development of coupled thermal-hydraulic / neutronic models for the analysis of transients that are relevant in the safety analysis of the Swedish NPPs, and, in this framework, efforts in validating the U.S. NRC 3-D core neutronics simulator PARCS [1, 2, 3] were initiated. More specifically, PARCS models were developed for the Ringhals NPP - Unit 3 (a PWR core type) and for the Forsmark NPP - Unit 2 (a BWR core type). Then static calculations at different operating conditions were performed by making use of these two models, and the results were compared to the radial power distributions and the axial power profiles reconstructed from the in-core measurements provided by the owners of the plants.

The present document is organized as follows. In section 2, the two PARCS models are described. In section 3, the results from the assessment work are presented and discussed. Finally, in section 4, conclusions are drawn.

2. PARCS MODELLING

For the PARCS simulation of the neutronic behavior of a reactor core, one needs to prepare:

- a card name based input deck in which the calculation options and the core geometry and nodalization are specified;
- the PMAXS files that contains the data from which the neutron cross-sections and kinetic parameters can be obtained; and
- a file that contains the 3-dimensional spatial distribution of the history variables (burnup inclusive) and, in the present case, the instantaneous variables that identify the reactor core conditions at which the neutron cross-sections and kinetic parameters must be estimated.

2.1 Description of the card name based input files

Following the guidelines provided by the PARCS User's Manual [3], two input decks were developed for describing the Ringhals-3 and the Forsmark-2 cores, respectively.

2.1.1 Ringhals-3 reactor model

The Ringhals-3 core consists of 157 fuel assemblies, and each of them is modeled with 26 axial levels, and, divided radially into 2 x 2 nodes. The first and the last axial levels are used for the bottom and top reflectors, respectively. As regards the radial reflector, 64 reflector 'assemblies' are employed and they surround radially the active core. These 64 reflector assemblies are of two types: the ones that only take the baffle in account, and the ones that include both the baffle and the core barrel.

Although control rods have no effect during normal operations (i.e., the control rods are completely withdrawn), they are also included since the present model is meant at investigating transient scenarios as well [4]. In the Ringhals-3 unit, all the control rods belong to the same type, and the different banks are defined on the basis of the different movements that groups of control rods can do.

Among those options that are used for the solution of the neutronic problem in PARCS, the boundary conditions for the neutron field are settled by assuming to zero incoming current. In addition, the PARCS hybrid neutronic solver based on a combination between an Analytic Nodal Method (ANM) and a Nodal Expansion Method (NEM) is selected.

2.1.2 Forsmark-2 reactor model

The nodalization used for the Forsmark-2 core is such that each of the 676 fuel assemblies is modeled radially with one node and axially with 27 equidistant nodes. Again, the first and the last axial levels are employed for the bottom and top reflectors, respectively. The other axial levels are such that the several different segments in which one fuel assembly is divided can be taken in account with little approximations. Besides, similarly to the PWR case, the radial reflector is reproduced by making use of dummy assemblies that surrounds the active core and that are associated to the proper radial reflector materials and conditions.

Then, since control rods in BWR play a role in normal operation, their modeling is also important for static predictions. In the Forsmark-2 core, there are 161 cruciform control rods, and they are of 5 different types. Since PARCS cannot model explicitly cruciform control rods, each control rod is defined as a bunch of 4 control rods placed in those fuel assemblies that are near the specific cruciform control rod. The 5 different types of control rods are modeled with the card 'CRB_DEF', the several banks of control rods and their location in the core are specified with the card 'BANK_CONF', the control rods positions are given in the card 'BANK_POS', and the type of control rods in each of the banks is provided in the card 'CRB_TYPE'.

As for the PWR model, zero incoming current is assumed as boundary condition for the neutron field, and a hybrid neutronic solver is used.

2.2 Cross-sections preparation and PMAXS files

In order to perform core calculations, material constants and kinetic parameters representative of the actual local conditions, of the exposure, and of the history effects for a specific core are needed. Such properties are provided to PARCS *via* proper files, so-called PMAXS files. These files can be generated from the 2-D transport calculations performed at fuel-assembly level with the HELIOS code [5] or the CASMO-4 code [6]. For this purpose, the separate core module GenPMAXS [7] was developed.

In the context of the work presented in this report, an alternative interface for building the PMAXS files was developed by the Division of Nuclear Engineering, Chalmers University of Technology, because data from HELIOS or CASMO-4 could not be released by the utilities. This novel approach is based on the capability of the Studsvik Scandpower 3-dimensional core simulator SIMULATE-3 [8] to retrieve, from binary library and restart files, all the material constants and kinetic parameters of all the fuel assemblies loaded in a specific core. Most importantly, the SIMULATE-3 code can then be used to edit any material/kinetic data for any fuel/reflector segment loaded in the considered core at any specified set of instantaneous and history variables. In such a way, the complete dependence of the material/kinetic data on instantaneous and history variables can be obtained. Therefore, no additional transport calculation is required, and the PMAXS files can be constructed relatively fast. Nevertheless, the procedure needs to take in account the fact that the CASMO-4/SIMULATE-3 formalism is different than the PARCS one, i.e., the data functionalization is different in the two cases.

In the following subsections, the Chalmers cross-section interface is described, the preparation of the cross-sections for the Ringhals-3 and Forsmark-2 cases is discussed, and the correct implementation of such a procedure is verified. More details on this topic (for the PWR case) can be found in reference [9].

2.2.1 Description of the Chalmers cross-section interface

As mentioned above, the CASMO-4/SIMUALTE-3 and the PARCS functionalizations of the cross-sections and of the neutron kinetic parameters with respect to the reactor core conditions differ from each other. Therefore, first, the two formalisms are introduced, and, then, the cross-section interface that was developed for the generation of the PMAXS files from the SIMULATE-3 library and restart files is described.

2.2.1.1 CASMO-4/SIMULATE-3 formalism

According to the CASMO-4/SIMULATE-3 model [10], the macroscopic and microscopic two-group cross-sections, discontinuity factors, fission product data and detector data can be expressed in a generic form as

$$P(A,B,C) = P(A_0,B_0,C_0) + \Delta P_A(A) + \Delta P_B(A,B) + \Delta P_C(A,B,C)$$

eq. 2-1

where $P(A_0,B_0,C_0)$ is the base value, and

$$\Delta P_A(A) = \int_{A_0}^{A} \frac{\partial}{\partial A'} P(A',B_0,C_0)dA'$$

eq. 2-2

$$\Delta P_B(A,B) = \int_{B_0}^{B} \frac{\partial}{\partial B'} P(A,B',C_0)dB'$$

eq. 2-3

$$\Delta P_C(A,B,C) = \int_{C_0}^{C} \frac{\partial}{\partial C'} P(A,B,C')dC'$$

eq. 2-4

The approach for the generation of this specific type of parameters *via* eqs. 2-1 to 2-4 is displayed in a more intuitive manner in Fig. 2-1.

In brief, the data needed in eq. 2-1 are obtained from CASMO-4 lattice calculations and organized into additive series of tables containing the partial functions. For those points of the tables in which data are not available, second-order Lagrangian interpolation is applied. Moreover, one can notice that, according to this scheme, parameters can only depend on a limited number of variables, i.e., no more than three variables are allowed. Tables 2-1 and 2-2 summarize the possible CASMO-4/SIMULATE-3 data functionalization in PWR cases and in BWR cases [11, 12], respectively.

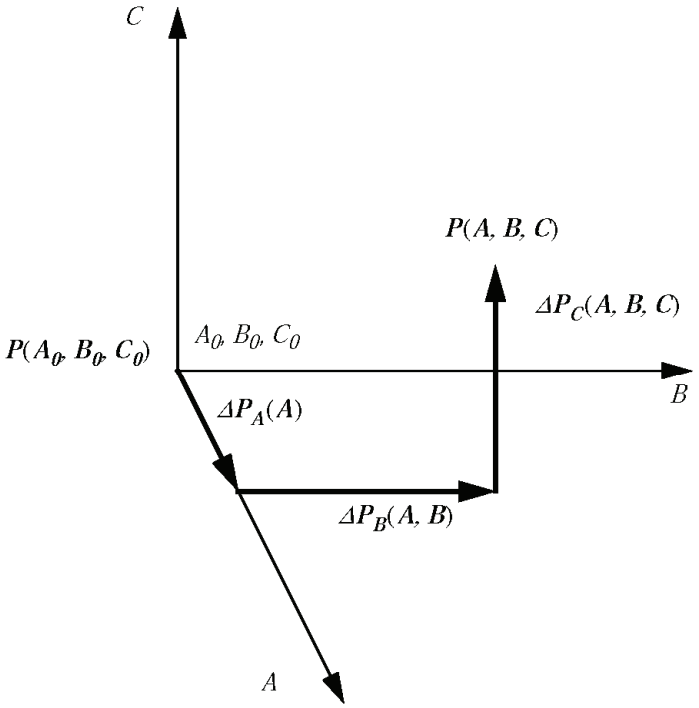

Figure 2-1 Construction of the macroscopic and microscopic two-group cross-sections, discontinuity factors, fission product data, and detector data in the CASMO-4/SIMULATE-3 code package

Table 2-1 CASMO-4/SIMULATE-3 data functionalization for PWR cases

Parameter P	Fuel segment	Reflector segment	
		Radial and bottom	Top
D_1, D_2 $\Sigma_{1\to2}$ $\Sigma_{a,1}$, $\Sigma_{a,2}$ $\nu\Sigma_{\mathrm{f},1}$, $\nu\Sigma_{\mathrm{f},2}$ κ/ν $\sigma_{a,1}^{B^{10}}$, $\sigma_{a,2}^{B^{10}}$	$P(b, HT_m) + \Delta P_{HC_b}(b, HC_b) + \Delta P_{C_b}(b, C_b) + \Delta P_{T_m}(b, T_m) + \Delta P_{T_f}(b, T_f) + \Delta P_{\alpha_{CR}}(b, \alpha_{CR}) + \Delta P_{T_{cooling}}(b, T_{cooling})$ $[optionally, +\Delta P_{b_{BP}}(b, b_{BP})]$	$P(C_b)$	$P(C_b, T_m)$
ν $\gamma_{I^{135}}$, $\gamma_{Xe^{135}}$, $\gamma_{Pm^{149}}$, $\gamma_{Sm^{149}}$ $\sigma_{a,2}^{Xe^{135}}$, $\sigma_{a,2}^{Sm^{149}}$ Gd fraction remaining		-	-
discontinuity factors	$\Delta P_{C_b}(b, C_b) + \Delta P_{T_m}(b, T_m) + \Delta P_{T_f}(b, T_f) + \Delta P_{\alpha_{CR}}(b, \alpha_{CR}) + \Delta P_{T_{cooling}}(b, T_{cooling})$ $[optionally, +\Delta P_{b_{BP}}(b, b_{BP})]$	$P(C_b)$	$P(C_b, T_m)$

Table 2-2 CASMO-4/SIMULATE-3 data functionalization for BWR cases

Parameter P	Fuel segment	Reflector segment	
		Radial and bottom	Top
D_1, D_2 $\Sigma_{1\to2}$ $\Sigma_{a,1}$, $\Sigma_{a,2}$ $\nu\Sigma_{\mathrm{f},1}$, $\nu\Sigma_{\mathrm{f},2}$ κ/ν $\sigma_{a,1}^{B^{10}}$, $\sigma_{a,2}^{B^{10}}$	$P(b,H\alpha)+\Delta P_{\alpha}(b,H\alpha,\alpha)$ $+\Delta P_{T_f}(b_{RES},T_f)$ $+\Delta P_{\alpha_{CR}}(b_{RES},\alpha_{CR})$ $+\Delta P_{H\alpha_{CR}}(b,\alpha_{CR},H\alpha_{CR})$ $+\Delta P_{T_{cooling}}(b,T_{cooling})$	$P(T_m)$	$P(\alpha)$
ν $\gamma_{I^{135}}$, $\gamma_{Xe^{135}}$, $\gamma_{Pm^{149}}$, $\gamma_{Sm^{149}}$ $\sigma_{a,2}^{Xe^{135}}$, $\sigma_{a,2}^{Sm^{149}}$ Gd fraction remaining		-	-
discontinuity factors	$P(b,H\alpha)+\Delta P_{\alpha}(b_{RES},\alpha)$ $+\Delta P_{T_f}(b_{RES},T_f)$ $+\Delta P_{\alpha_{CR}}(b_{RES},\alpha,\alpha_{CR})$ $+\Delta P_{T_{cooling}}(b,T_{cooling})$	$P(T_m)$	$P(\alpha)$
Fission rate of U-235 in detector position Peaking factor	$P(b,H\alpha)+\Delta P_{\alpha}(b_{RES},\alpha)$ $+\Delta P_{T_f}(b_{RES},T_f)$ $+\Delta P_{\alpha_{CR}}(b_{RES},\alpha,\alpha_{CR})$	-	-

In addition, for those quantities for which the principal variation is due to burnup, like,

- pin-by-pin power distribution,
- corner flux ratios,
- detector flux,
- peaking factors,
- detector microscopic cross-sections,
- two-group neutron velocities,
- effective neutron precursor yields, and
- precursor decay constants,

one-dimensional table sets in exposure are given. The additional dependencies are modeled with one-dimensional tables of the derivatives of the data as function of the exposure. Thus, the model applied in this case is as follows [10],

$$P(b, B, C, \dots, Z) = P(b, B_0, C_0, \dots, Z_0) + \Delta P_B(b) + \Delta P_C(b) + \cdots + \Delta P_Z(b)$$

eq. 2-5

where b is the exposure (burnup), and

$$\Delta P_B(b) = \int_{B_0}^{B} \frac{\partial}{\partial B'} P(b, B', C_0, \dots, Z_0) dB'$$

eq. 2-6

$$\Delta P_C(b) = \int_{C_0}^{C} \frac{\partial}{\partial C'} P(b, B_0, C', \dots, Z_0) dC'$$

eq. 2-7

$$\Delta P_Z(b) = \int_{Z_0}^{Z} \frac{\partial}{\partial Z'} P(b, B_0, C_0, \dots, Z') dZ'$$

eq. 2-8

The variables $A, B, C, \ldots, Z$ that appear in eq. 2-5 depend on the case that is studied and they can be, besides burnup b,

- fuel temperature T_f;
- history-averaged fuel temperature HT_f;
- moderator temperature T_m;
- history-averaged moderator temperature HT_m;
- void fraction α;
- history-averaged void fraction $H\alpha$;
- boron concentration C_b;
- history-averaged boron concentration HC_b;
- control rod insertion α_{CR};
- history-averaged control rod insertion $H\alpha_{CR}$;
- burnable absorber exposure b_{BP}; and
- $T_{cooling}$ for the shutdown decay time.

2.2.1.2 PARCS formalism

In the case of PARCS, any generic parameter P (that could represent a macroscopic cross-section, a microscopic cross-section, an assembly discontinuity factor, a kinetic parameter, etc.) can be written as [2, 7],

$$\begin{aligned} P\left(b, H, \alpha_{CR}, D_m, C_b, T_f, T_m\right) &= P\left(b, H, \alpha_{CR,0}, D_{m,0}, C_{b,0}, T_{f,0}, T_{m,0}\right) + \left.\frac{\partial P}{\partial \alpha_{CR}}\right|_{\left(b,H,\alpha_{CR,ref}\right)} \left(\alpha_{CR} - \alpha_{CR,0}\right) \\ &+ \left.\frac{\partial P}{\partial D_m}\right|_{\left(b,H,\alpha_{CR},D_{m,ref}\right)} \left(D_m - D_{m,0}\right) + \left.\frac{\partial P}{\partial C_b}\right|_{\left(b,H,\alpha_{CR},D_m,C_{b,ref}\right)} \left(C_b - C_{b,0}\right) \\ &+ \left.\frac{\partial P}{\partial \sqrt{T_f}}\right|_{\left(b,H,\alpha_{CR},D_m,C_b,T_{f,ref}\right)} \left(\sqrt{T_f} - \sqrt{T_{f,0}}\right) \\ &+ \left.\frac{\partial P}{\partial T_m}\right|_{\left(b,H,\alpha_{CR},D_m,C_b,T_f,T_{m,ref}\right)} \left(T_m - T_{m,0}\right) \end{aligned}$$

eq. 2-9

where

- b is the burnup;
- H is either one history variable or a vector of two history variables;
- α_{CR} is the effective rodded fraction;
- D_m is the moderator density;
- C_b is the boron concentration;
- T_f is the effective fuel temperature; and
- T_m is the moderator temperature.

The subscript 0 denotes the base case, and the subscript ref the reference point that is defined as the midpoint between the instantaneous value and the base value.

It must be borne in mind that PARCS, at the time when the cross-section interface was developed, could not handle more than 2 history variables.

The partial derivatives that appear in eq. 2-9 can be estimated as,

$$\left.\frac{\partial P}{\partial v}\right|_{(u,v_{ref})} = \frac{P(u,v,w_0) - P(u,v_0,w_0)}{v - v_0}$$

eq. 2-10

where

- u represents all the variables having their instantaneous values; and
- w_0 represents all the variables having their base values.

In addition, according to the PARCS formalism, the data related to each of the parameters are stored into a three levels structure, each level having a 'tree-leave' structure (an example for a PWR case is shown in Fig. 2-2). The highest level represents the history cases. The second level in the PARCS structure is related to the different possible instantaneous states of variables as the control rod insertion, moderator density, boron concentration, fuel temperature, etc., for each history case. In the third level the burn-up dependency of the data can be reproduced. Therefore, when any parameter is needed by PARCS at a given set of operating conditions, the data are retrieved from the tree-leave formalism, and used through eqs. 2-9 and 2-10.

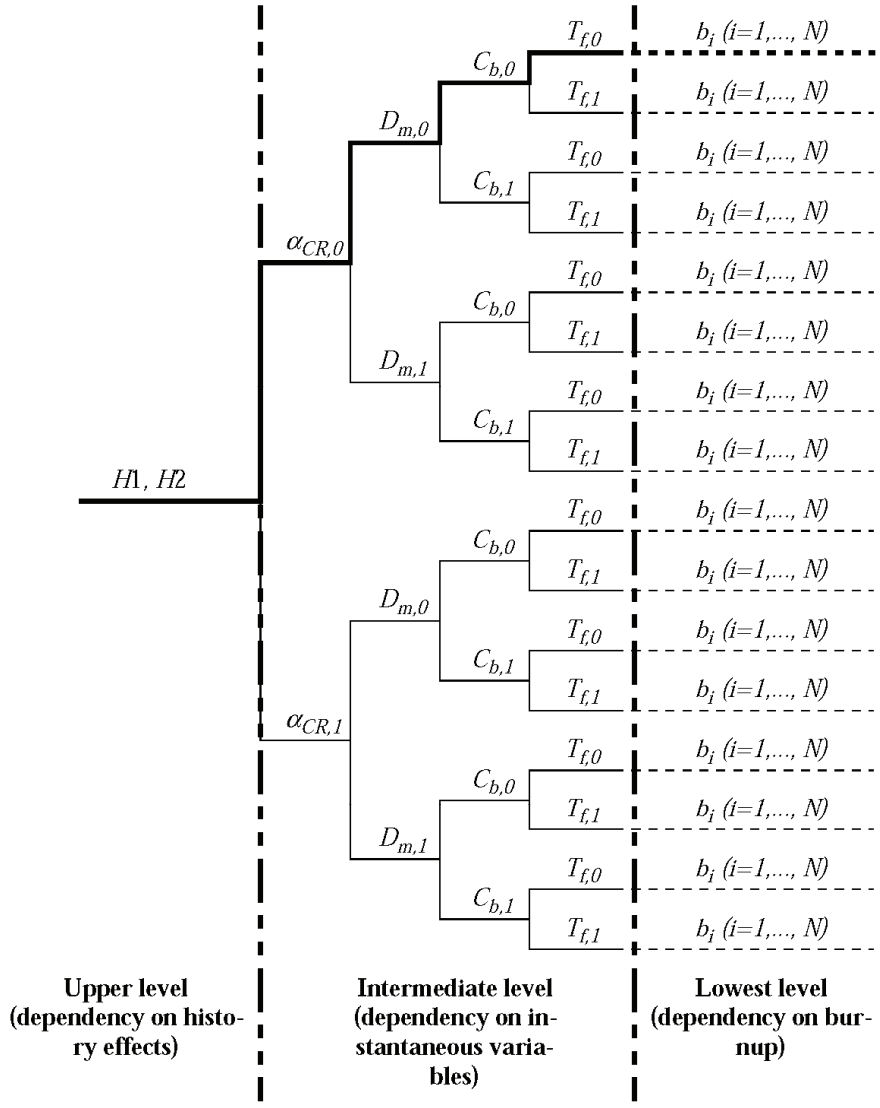

Figure 2-2 ”Tree-leave” formalism in PARCS for PWR cases (the subscript 0 denotes the base case, the subscript 1 the perturbed value). The last ramification about the burnup dependency is not explicitly displayed for reason of clarity of the chart

2.2.1.3 Description of the Chalmers cross-section interface

The Chalmers cross-section interface developed to build-up the PMAXS files consists of 3 steps.

In the first step, the fuel/reflector assemblies loaded in the core are retrieved from the SIMULATE-3 restart file, and the operating points (i.e. instantaneous and history conditions, burnup inclusive) at which the material/kinetic data are available are also extracted from the SIMULATE-3 library file. More specifically, the following data are gathered into a summary file:

- the segment number, its name, the type of segment (i.e., fuel or reflector), the number of rods, the number of heated rods, the average enrichment;
- the burnup points;
- the instantaneous values and the histories for the fuel temperature, moderator density/temperature, boron concentration, and control rod position, as well as which points are referred to as base condition or branch; and
- the shutdown cooling times, and whether these points are referred to as base conditions or branches.

In the second step, the data contained in the summary file are edited according to the PARCS 'tree-leave' formalism discussed in subsection 2.2.2, and stored in a SIMULATE-3 output file. As mentioned above, this 'tree-leave' structure does not correspond to the way the data are functionalized in CASMO-4/SIMULATE-3 (see subsection 2.2.1). Nevertheless, the SIMULATE-3 interpolation procedure can be used with confidence for following each branch of the PARCS 'tree-leave' structure and then editing the corresponding data.

In the third and last step, the PMAXS files are built for each of the fuel/reflector segments. This is done by successively stacking the results of different sets of values for the history variables. For each set of values for the history variables, the results corresponding to the 'base' branch are first stored for each burnup point. The partial derivatives associated to each instantaneous variable are then computed for each branch associated to a change of the considered instantaneous variable according to eq. 2-10 and for each burnup point. When constructing the PMAXS files, care has to be taken about the transport cross-sections and the macroscopic thermal absorption cross-sections. The transport cross-sections, which it is not directly given by SIMULATE-3, is derived from the diffusion coefficients D_i as follows,

$$\Sigma_{tr,i} = \frac{1}{3D_i}$$

eq. 2-11

As regards the thermal absorption cross-section $\Sigma_{a,2}$, the effect of the Xe-135 and Sm-149 poisons might be included. This is the case when the SIMULATE-3 libray file is created with equilibrium fission products [13]. However, in a PARCS calculation (and, especially, when the concentration of the poisons is different from the equilibrium one), PARCS itself will provide the concentration of the poisons explicitly. Thus, the effect of the poisons in the thermal absorption

cross-section retrieved from SIMULATE-3 has to be removed, i.e.

$$\Sigma_{a,2}^{without\ poisons} = \Sigma_{a,2}^{with\ poisons} - \left(N_{Xe^{135}}\sigma_{a,2}^{Xe^{135}} + N_{Sm^{149}}\sigma_{a,2}^{Sm^{149}}\right)$$

eq. 2-12

The current interface has also some limitations, i.e. some data cannot be retrieved, such as

- the kinetic data (precursor decay constants, fractions of delayed neutrons, inverse velocities) for individual fuel assemblies;
- the corner discontinuity factors;
- the power form factors.

2.2.2 Preparation of PARCS cross-sections for the Ringhals-3 PWR unit

For the Ringhals-3 core, the PARCS data functionalization of any parameter P related to any fuel segment is based on:

- the burnup b,
- the history of the moderator density HD_m,
- the history of the boron concentration HC_b,
- the instantaneous boron concentration C_b,
- the instantaneous effective fuel temperature T_f,
- the instantaneous moderator density D_m, and
- the effective rodded fraction α_{CR}.

Therefore eq. 2-9 becomes,

$$\begin{aligned} P\left(b, HD_m, HC_b, \alpha_{CR}, D_m, C_b, T_f\right) &= P\left(b, HD_{m,0}, HC_{b,0}, \alpha_{CR,0}, D_{m,0}, C_{b,0}, T_{f,0}, T_{m,0}\right) \\ &+ \left.\frac{\partial P}{\partial \alpha_{CR}}\right|_{\left(b,HD_m,HC_b,\alpha_{CR,ref}\right)} \left(\alpha_{CR} - \alpha_{CR,0}\right) + \left.\frac{\partial P}{\partial D_m}\right|_{\left(b,HD_m,HC_b,\alpha_{CR},D_{m,ref}\right)} \left(D_m - D_{m,0}\right) \\ &+ \left.\frac{\partial P}{\partial C_b}\right|_{\left(b,HD_m,HC_b,\alpha_{CR},D_m,C_{b,ref}\right)} \left(C_b - C_{b,0}\right) \\ &+ \left.\frac{\partial P}{\partial \sqrt{T_f}}\right|_{\left(b,HD_m,HC_b,\alpha_{CR},D_m,C_b,T_{f,ref}\right)} \left(\sqrt{T_f} - \sqrt{T_{f,0}}\right) \end{aligned}$$

eq. 2-13

For the reflector segments, the parameters P is functionalized only with respect to the instantaneous value of the boron concentration, i.e.,

$$P(C_b) = P(C_{b,0}) + \left.\frac{\partial P}{\partial C_b}\right|_{(C_{b,ref})} (C_b - C_{b,0})$$

eq. 2-14

Although the cross-section interface discussed in subsection 2.2.3 allows retrieving the dependency of the reflector material data on the instantaneous moderator density as well, such dependency is not used because the necessary data are not available in the SIMULATE-3 summary file that is used for PARCS static calculations (see subsection 2.3) [14].

2.2.3 Preparation of PARCS cross-sections for the Forsmark-2 BWR unit

In the case of the Forsmark-2 model, history of void fraction $H\alpha$ and history of control rod insertion $H\alpha_{CR}$ are chosen to be the two history variables in the PARCS functionalization of the parameters P for the fuel segments, together with the instantaneous effective fuel temperature, the instantaneous moderator density, and the instantaneous effective rodded fraction. For this specific application, eq. 2-9 can then be reduced to:

$$\begin{aligned} P(b, H\alpha, H\alpha_{CR}, \alpha_{CR}, D_m, T_f) \\ = P(b, HD_{m,0}, HC_{b,0}, \alpha_{CR,0}, D_{m,0}, , T_{f,0}) + \left.\frac{\partial P}{\partial \alpha_{CR}}\right|_{(b,HD_m,HC_b,\alpha_{CR,ref})} (\alpha_{CR} - \alpha_{CR,0}) \\ + \left.\frac{\partial P}{\partial D_m}\right|_{(b,HD_m,HC_b,\alpha_{CR},D_{m,ref})} (D_m - D_{m,0}) \\ + \left.\frac{\partial P}{\partial \sqrt{T_f}}\right|_{(b,HD_m,HC_b,\alpha_{CR},D_m,C_b,T_{f,ref})} \left(\sqrt{T_f} - \sqrt{T_{f,0}}\right) \end{aligned}$$

eq. 2-15

As regards the parameters P that characterize the reflector segments, they are computed by only taking in account the instantaneous moderator density, as follows,

$$P(D_m) = P(D_{m,0}) + \left.\frac{\partial P}{\partial D_m}\right|_{(D_{m,ref})} (D_m - D_{m,0})$$

eq. 2-16

2.2.4 Verification of the Chalmers cross-section interface

Before using the cross-section interface for practical applications, it was verified that PARCS can correctly reconstruct the data from the PMAXS files generated with such an interface. For that purpose, all the possible combinations of values of instantaneous and history variables appearing in the PMAXS files were employed as sets of operating conditions for PARCS calculations. Thus, the data reconstructed from the PMAXS files, according to eq. 2-9, for each of the calculations, were compared with the data that were built from the SIMULATE-3 library file, according to eq. 2-1.

The procedure for the verification process can be summarized as follows. First, data are retrieved from the SIMULATE-3 library file, for all the possible combinations of values of the instantaneous variables, of the history variables, and of burnup. Thereafter, the PARCS input files for each set of variables are built-up. In particular, each of the PARCS input files models only one assembly through a pseudo-assembly, where segments covering the whole range of exposure were axially stacked, so that the whole dependency of the material data on burnup can be handled in one single calculation and computational effort can be saved. On the other hand, the moderator density, fuel temperature, boron concentration, etc. are kept constant in each input file. Finally, from each of the PARCS runs, the material data are edited at the corresponding values of burnup, instantaneous variables, and history variables, for a single segment, and compared to the original data directly coming from the SIMULATE-3 binary file.

In the case of PWR applications, the verification procedure was applied fully, and, for the sake of simplicity, the results achieved for only a few combinations of instantaneous and history variables are shown in Fig. 2-3. By comparing the infinite multiplication factor calculated with the SIMULATE-3 cross-sections and with the PARCS cross-sections (i.e. the cross-sections from the PMAXS files generated with the new interface), one can find an excellent agreement between the two cases, and conclude that the Chalmers cross-section interface works correctly.

As regards BWR applications, only a random check was performed for verifying that PARCS retrieves the correct data from SIMULATE-3:

- detector flux, for the base history, one history of moderator density, and one history of the control rod position;
- on each of the histories, for the reference branch, a few control rod branches, a few moderator density branches, and a few fuel temperature branches; and
- on each of the branches, for two random burnup points.

Again, the data reconstructed by PARCS matched the original data, and the correct implementation of the interface could thus be demonstrated for BWR applications as well.

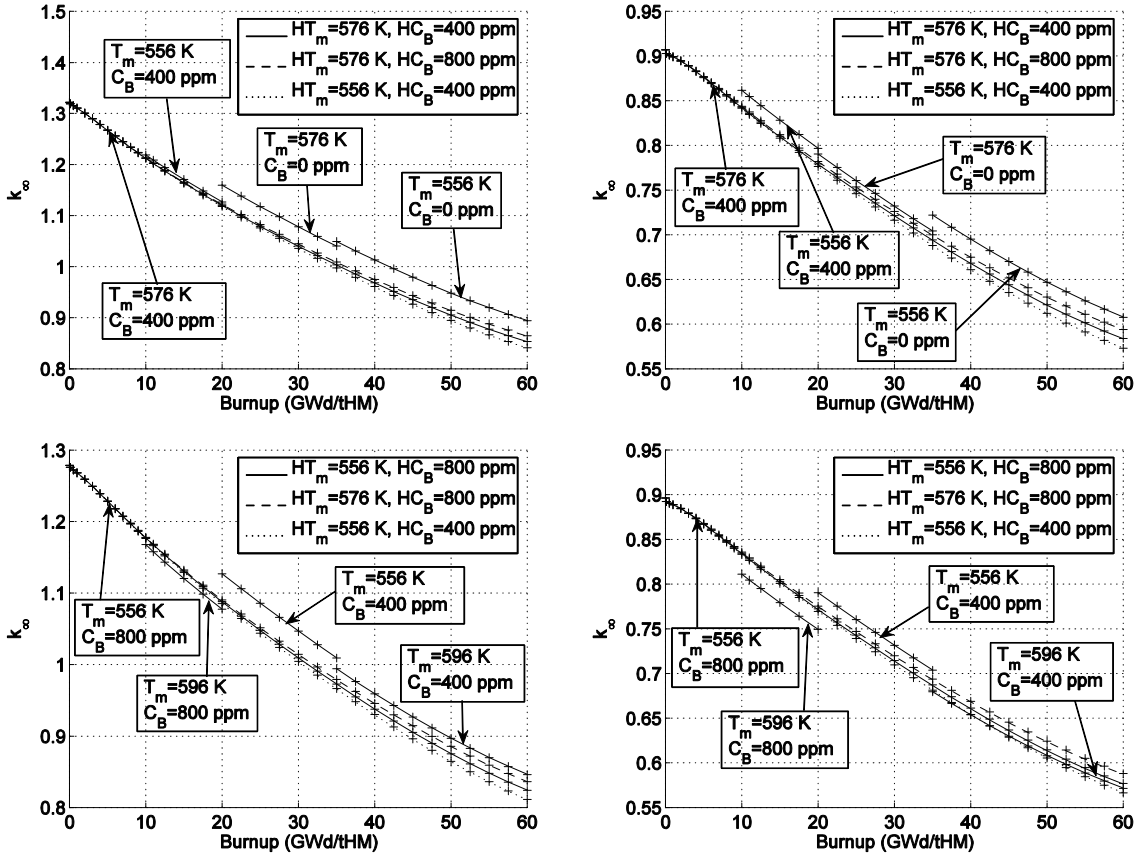

Figure 2-3 PWR case, variation of k_∞ as a function of burnup, instantaneous and history variables. The infinite multiplication factor calculated from the original data is represented by lines, whereas the infinite multiplication factor calculated from the reconstructed data is represented by crosses

2.3 3-D distribution of the history and instantaneous variables

In order to run a static core calculation with PARCS, 3-D distribution of the history and instantaneous variables must be available, so that cross-sections and neutron kinetic parameters can be evaluated at the proper local conditions. Former SIMULATE-3 calculations were performed for the same reactor core conditions of interest as in the current work. Thereafter, the SIMULATE summary files from these simulations were properly modified and directly used as spatial distributions of both history and instantaneous variables fed to PARCS (see the description of the PARCS card 'INP_HST' in [3]). However, it must be mentioned that PARCS has also the capability to calculate the spatial distribution of the moderator density and of the fuel temperature over the core. Such a capability was not used in the present work.

On the contrary, the concentration of the poisons was recalculated by PARCS, based on the corresponding microscopic cross-sections and fission yields stored in the PMAXS files, by activating the PARCS card 'XE_SM'.

3. RESULTS OF THE STATIC CALCULATION AND COMPARISONS WITH MEASUREMENT DATA

Several sets of measured data at different core exposures and for different fuel cycles were available for the Swedish Ringhals-3 PWR unit and the Forsmark-2 BWR unit. In the Ringhals unit 3, the neutron flux measurements were carried out by making use of Movable In-Core (MIC) detectors, which are fission chambers. These detectors can only be positioned in the central instrumentation tube of a limited number of assemblies. In the Forsmark unit 2, neutron flux measurements are given by Traversing Incore Prove (TIP) detectors that are located in a certain number of inter-assembly instrumentation tubes. For both cases detector signals can be used in SIMULATE-3 to reconstruct the Relative Power Fraction (RPF) for each of the nodes in which the reactor core has been discretized for the solution of the neutronic equations.

In order to evaluate the accuracy of the static calculations, the values of the RPF estimated with SIMULATE-3 from the detector signals are thus compared against the values predicted by PARCS, node by node, in terms of relative differences, as follows:

$$\Delta = \frac{RPF_{PARCS} - RPF_{measured}}{RPF_{measured}} \qquad \text{eq. 3-1}$$

where

- RPF_{PARCS} is the RPF calculated with PARCS, for one core node; and
- $RPF_{measured}$ is the RPF estimated by SIMULATE-3 from the detector signals, for one core node.

3.1 PWR case

The cases studied for Ringhals-3 are summarized in Table 3-1. The sets of measurements correspond to three different fuel cycles, and, for each cycle, they referred to operating conditions at about the beginning, the middle and the end of the cycle (except for cycle 22 for which measured data at the end of the cycle were not available).

Table 3-1 Ringhals-3 PWR unit, Operating conditions of the measurement sets

Fuel Cycle	**Exposure** [GWd/tHM]	**Relative Power** [%]	**Core-averaged Coolant Temperature** [°C]	**Critical Boron Concentration** [ppm]
10	0.2208	99.8	303.3	965
10	4.8136	99.8	303.0	524
10	9.5929	99.8	303.2	79
19	0.3694	100.0	301.4	915
19	4.5983	100.0	301.4	519
19	9.830	100.1	301.2	25
22	0.1442	99.1	301.2	1270
22	4.6668	100.1	301.3	828

The results are reported in details only for the fuel cycle 19, since similar trends can be observed for the others. The simulations shown in the following are computed with PARCS version 2.71. Nevertheless, the discussion is still valid for PARCS version 3.0, since almost identical predictions can be obtained (see Figs. 3-1 and 3-2).

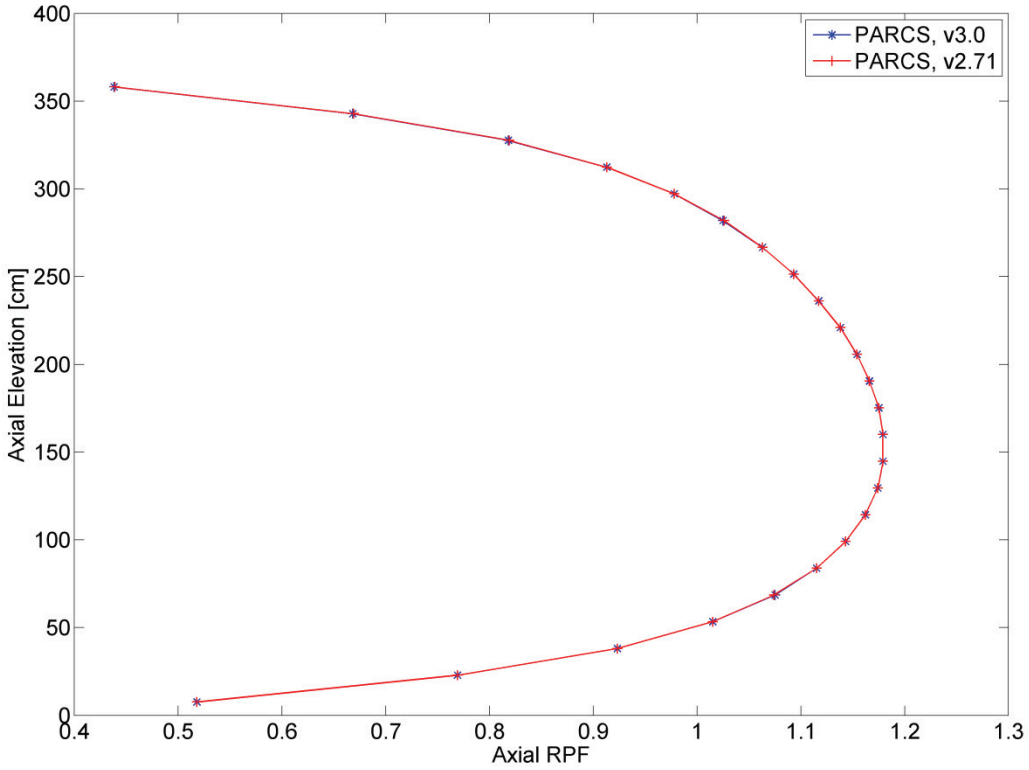

Figure 3-1 Ringhals-3 PWR unit, fuel cycle 19, exposure 0.3694 GWd/tHM: axial power profile calculated with PARCS version 3.0 and version 2.71

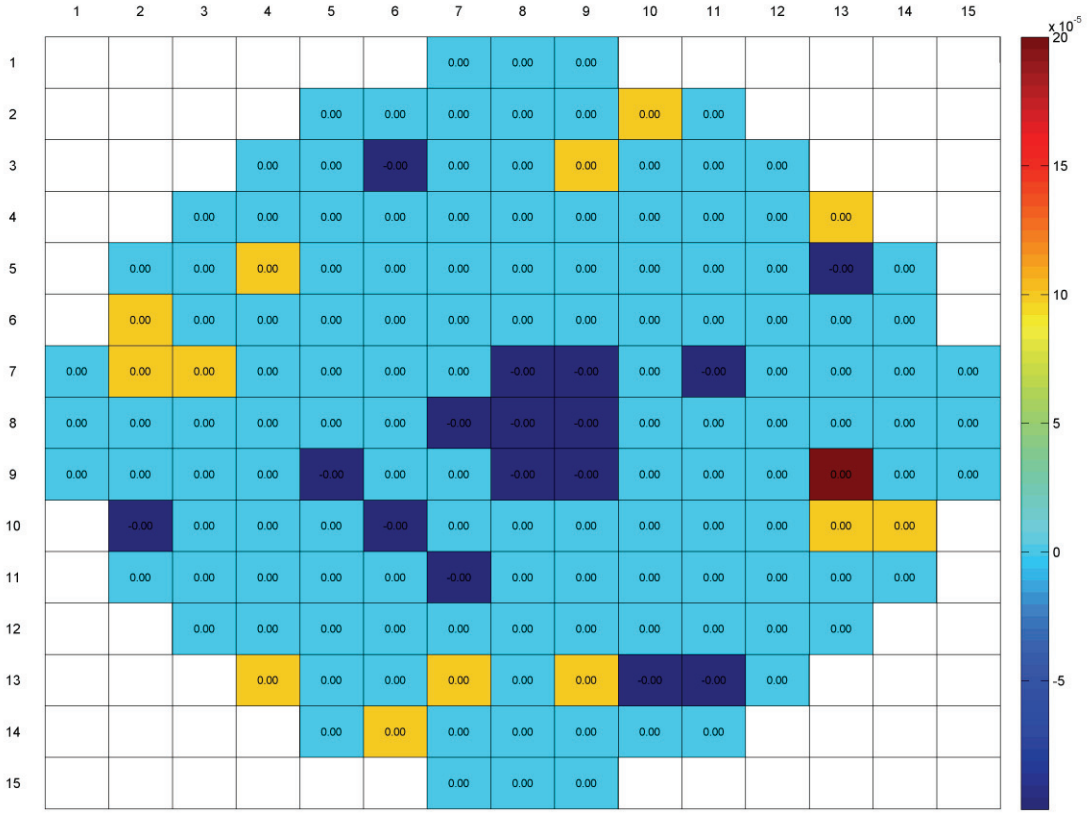

Figure 3-2 Ringhals-3 PWR unit, fuel cycle 19, exposure 0.3694 GWd/tHM: differences between the assemblywise radial power fraction calculated with PARCS version 3.0 and version 2.71

Figures 3-3 to 3-5 show the comparison between the axial power calculated with PARCS and the profile estimated from the measured data. A systematic deviation of the PARCS predictions from the measurements can be seen. As mentioned in subsection 2.2.3, the variation of the cross-sections and neutron kinetic parameters in the reflector region due to the instantaneous moderator density is not included. This approximation might not be valid and can lead to a poor estimation of the axial leakage of neutrons through the top and bottom reflectors. Therefore, this fact could explain the larger discrepancy observed close to the top and the bottom of the active core. Nevertheless, the overall axial power profile is correctly reproduced by the PARCS simulations.

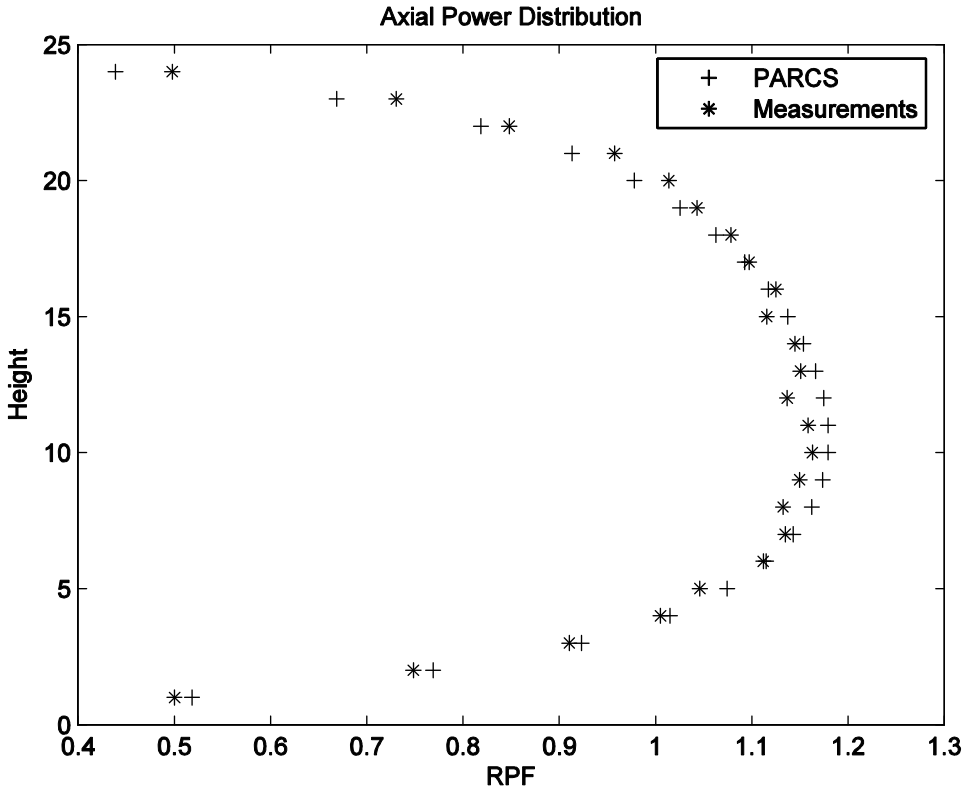

Figure 3-3 Ringhals-3 PWR unit, fuel cycle 19, exposure 0.3694 GWd/tHM: axial power profile

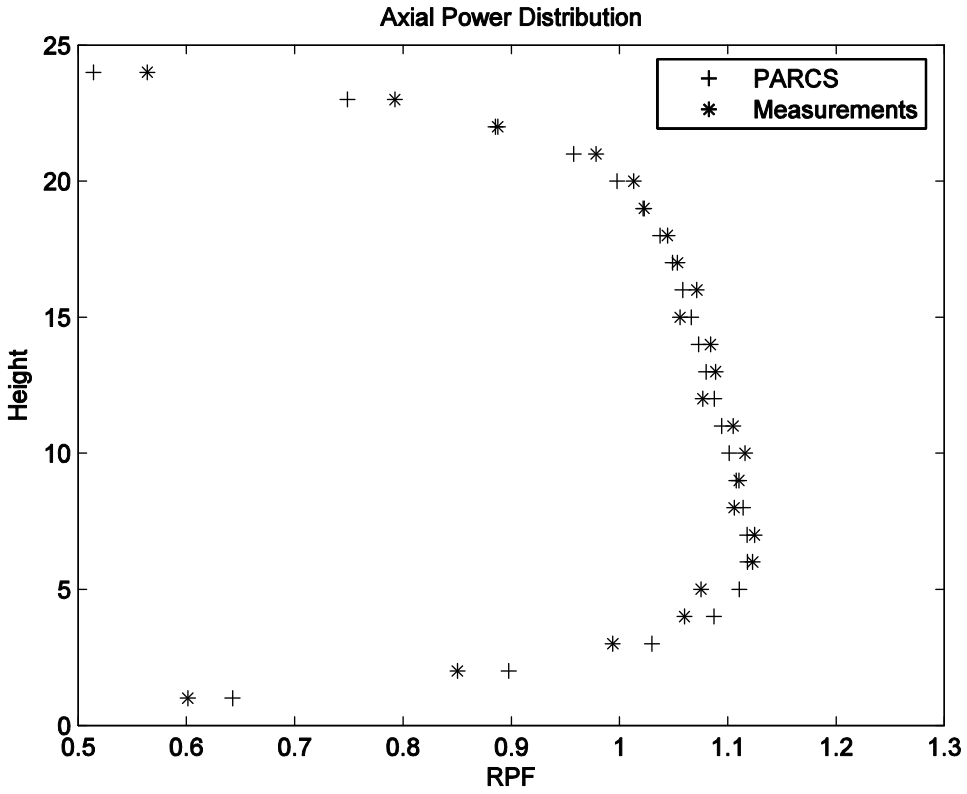

Figure 3-4 Ringhals-3 PWR unit, fuel cycle 19, exposure 4.5983 GWd/tHM: axial power profile

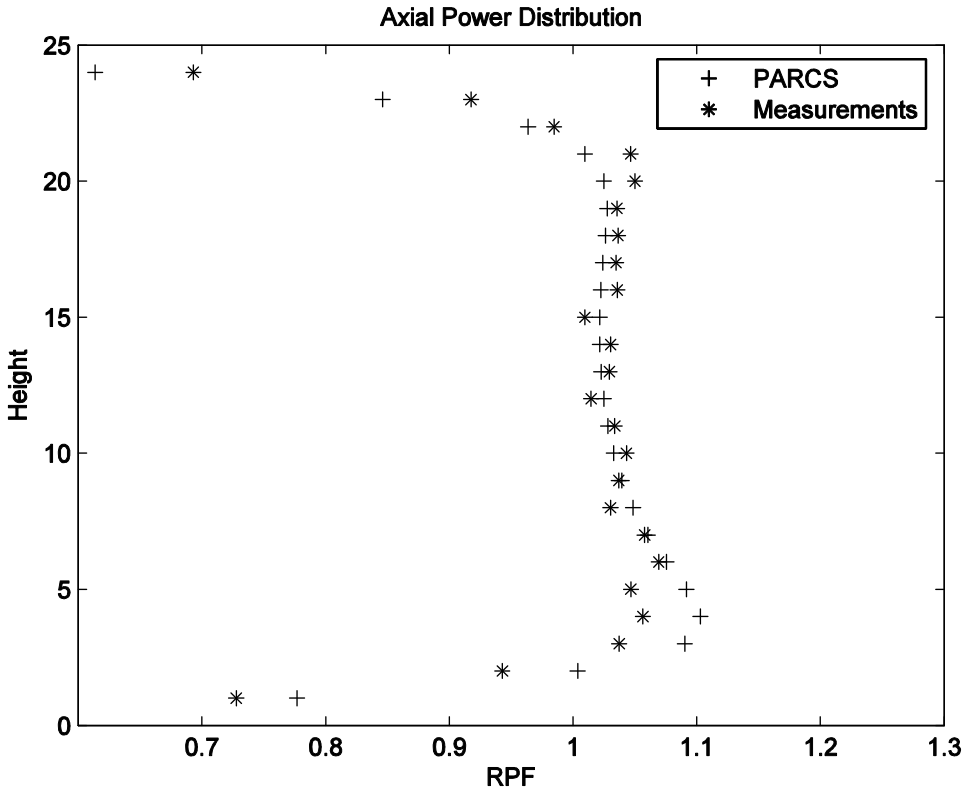

Figure 3-5 Ringhals-3 PWR unit, fuel cycle 19, exposure 9.830 GWd/tHM: axial power profile

As regards the radial power distribution, a trend can be identified by looking at the relative differences computed with eq. 3-1. At beginning of cycle conditions, the PARCS simulations overestimate the power in the center of the core and underestimate the power at the periphery (see Fig. 3-6). At middle of cycle conditions, the deviation of the PARCS results from the measured data does not exhibit any systematic behavior (see Fig. 3-7). At end of cycle, the calculations show an underestimation in the center of the core and an overestimation at the periphery (see Fig. 3-8).

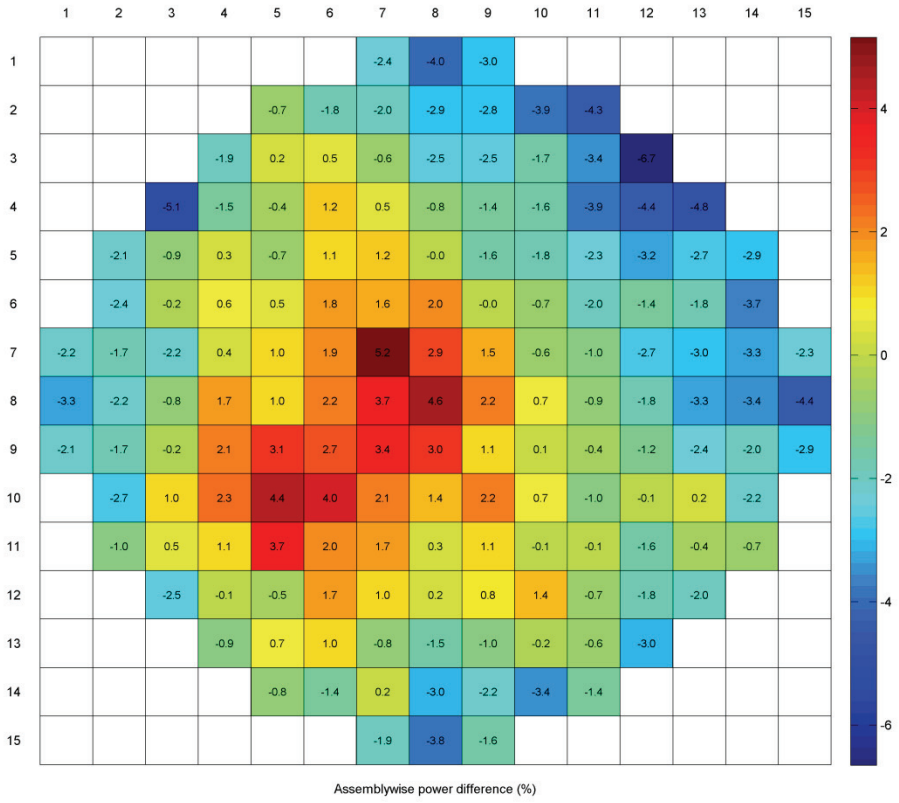

Figure 3-6 Ringhals-3 PWR unit, fuel cycle 19, exposure 0.3694 GWd/tHM: radial RPF relative differences (%)

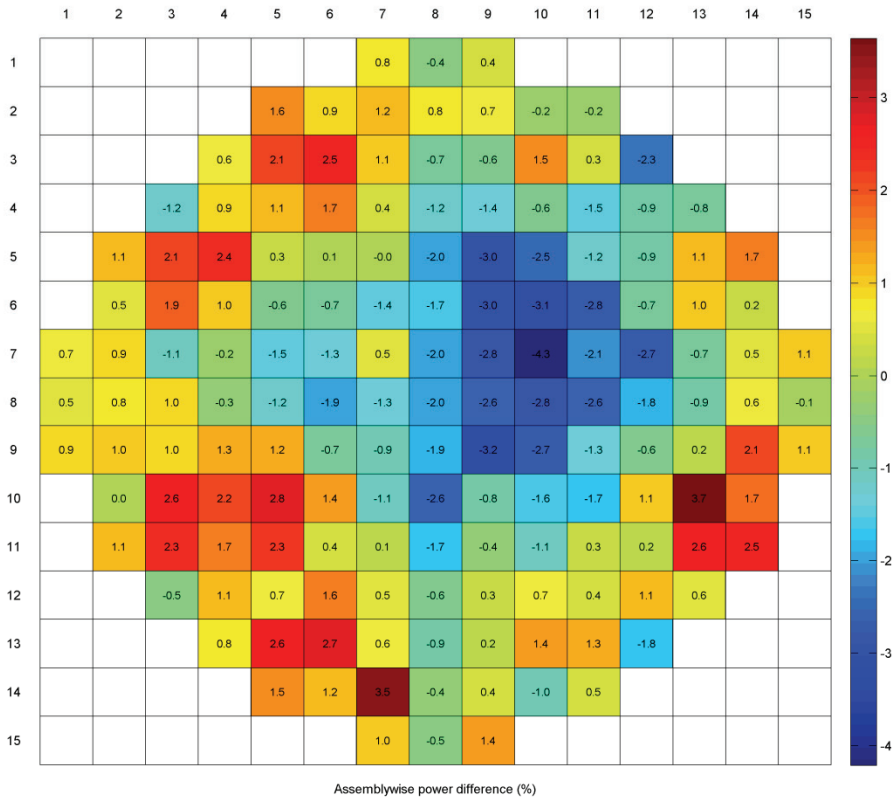

Figure 3-7 Ringhals-3 PWR unit, fuel cycle 19, exposure 4.5983 GWd/tHM: radial RPF relative differences (%)

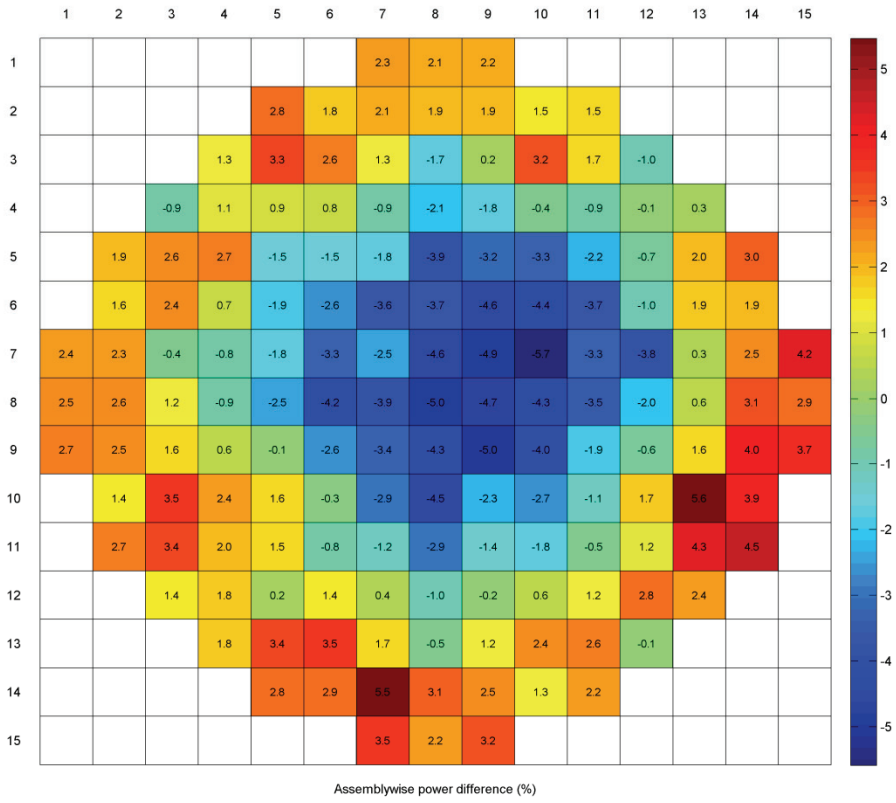

Figure 3-8 Ringhals-3 PWR unit, fuel cycle 19, exposure 9.830 GWd/tHM: radial RPF relative differences (%)

A summary of the relative differences between calculations and measurements for the several cases analyzed is reported in Table 3-2. It can be seen that the largest discrepancies are at the beginning and at the end of cycle, while the best performances can be found at the middle of cycle. Moreover, the effective multiplication factor k_{eff} shows a similar behavior, with a deviation from the expected criticality within typically 200 pcm.

Table 3-2 Ringhals-3 PWR unit, Summary of the assembly-wise deviations in power density

Fuel Cycle	Exposure [GWd/tHM]	Calculated k_{eff}	Relative difference between PARCS and measured relative power fraction (%)		
			Average	Minimum	Maximum
10	0.2208	0.99865	-0.91	-10.22	8.95
10	4.8136	1.00116	-0.21	-4.81	5.07
10	9.5929	1.00189	0.11	-5.14	7.01
19	0.3694	0.99986	-0.68	-6.72	5.25
19	4.5983	1.00052	0.02	-4.27	3.70
19	9.8300	1.00120	0.22	-5.67	5.56
22	0.1442	0.99764	-0.4	-5.10	5.79
22	4.6668	1.00017	0.17	-3.54	4.47

3.2 BWR case

The PARCS model of the Forsmark-2 BWR unit was compared against TIP measurements provided by Forsmark Kraftgrupp AB / Vattenfall Nuclear Fuel AB to Chalmers. The core operating conditions corresponding to these measurements are summarized in Table 3-3. This database includes the measurements performed in three different fuel cycles (21, 24, and 25), at about the beginning, the middle and the end of each cycle.

Table 3-3 Forsmark-2 BWR unit, Operating conditions of the measurements sets

Fuel Cycle	Exposure [GWd/tHM]	Relative Power [%]	Core-averaged Coolant Temperature [°C]
21	0.341	108	283.82
21	2.311	108.1	283.75
21	5.191	107.9	283.67
24	0.485	108.1	284.48
24	4.622	108.1	284.18
24	7.394	108	283.42
25	0.135	107.9	284.65
25	3.050	107.7	284.46
25	5.731	107.8	283.97

In the following discussion, only the results for the fuel cycle 21 are shown in details, since similar conclusions can be drawn for all the other cases. Besides, the calculations were performed with PARCS version 3.0. Nevertheless, as shown in Figs. 3-9 and 3-10, PARCS version 3.0 and version 2.71 produce simulations with negligible differences.

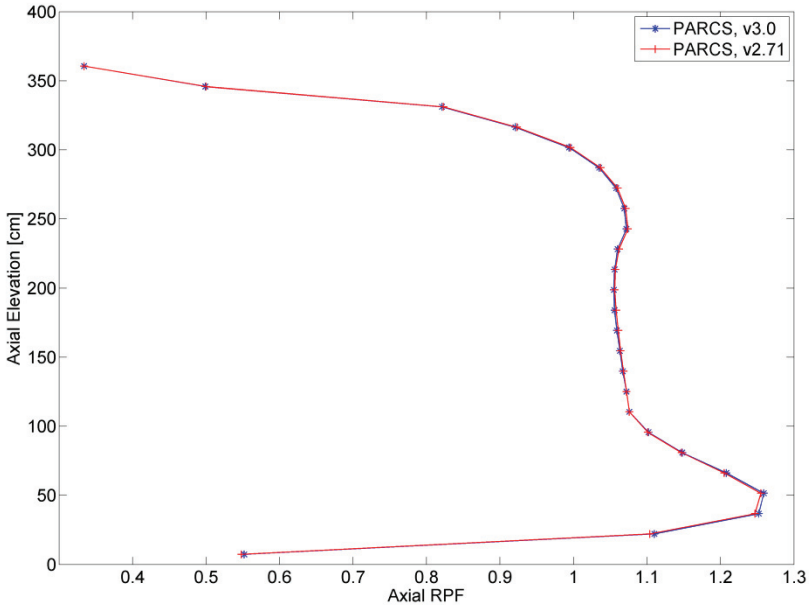

Figure 3-9 Forsmark-2 BWR unit, fuel cycle 21, exposure 0.341 GWd/tHM: axial power profile calculated with PARCS version 3.0 and version 2.71

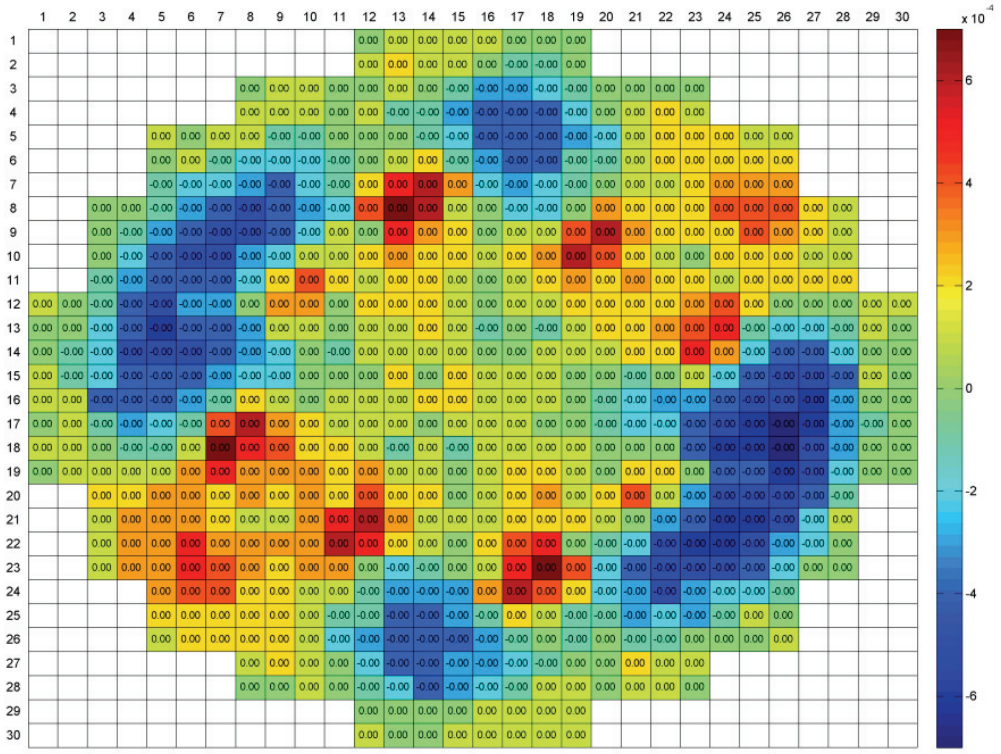

Figure 3-10 Forsmark-2 BWR unit, fuel cycle 21, exposure 0.341 GWd/tHM: differences between the assemblywise radial power fraction calculated with PARCS version 3.0 and version 2.71

Figures 3-11 to 3-13 display the positions of the control rods for the three operating conditions in cycle 21. Such control rods are moved through the fuel cycle, in order to compensate for the loss of reactivity that the core experiences during the life of one fuel load, and to keep the radial power distribution as flat as possible.

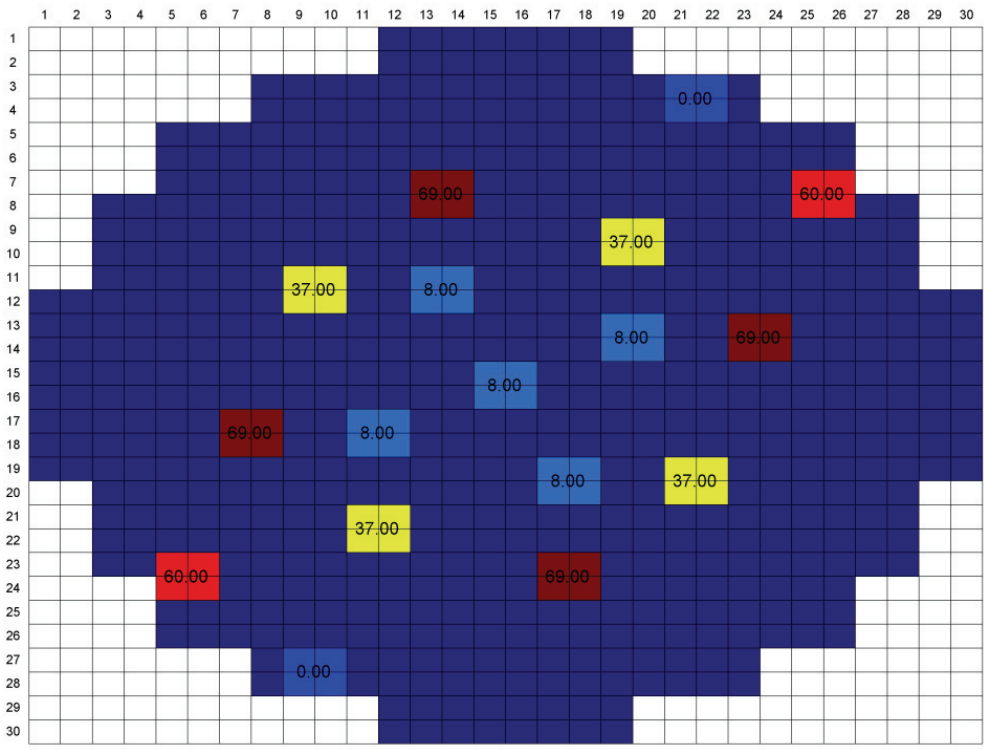

Figure 3-11 Forsmark-2 BWR unit, fuel cycle 21, exposure 0.341 GWd/tHM: control rods that are inserted and their positions in steps withdrawn ('100' is the value for a control rod that is completely withdrawn)

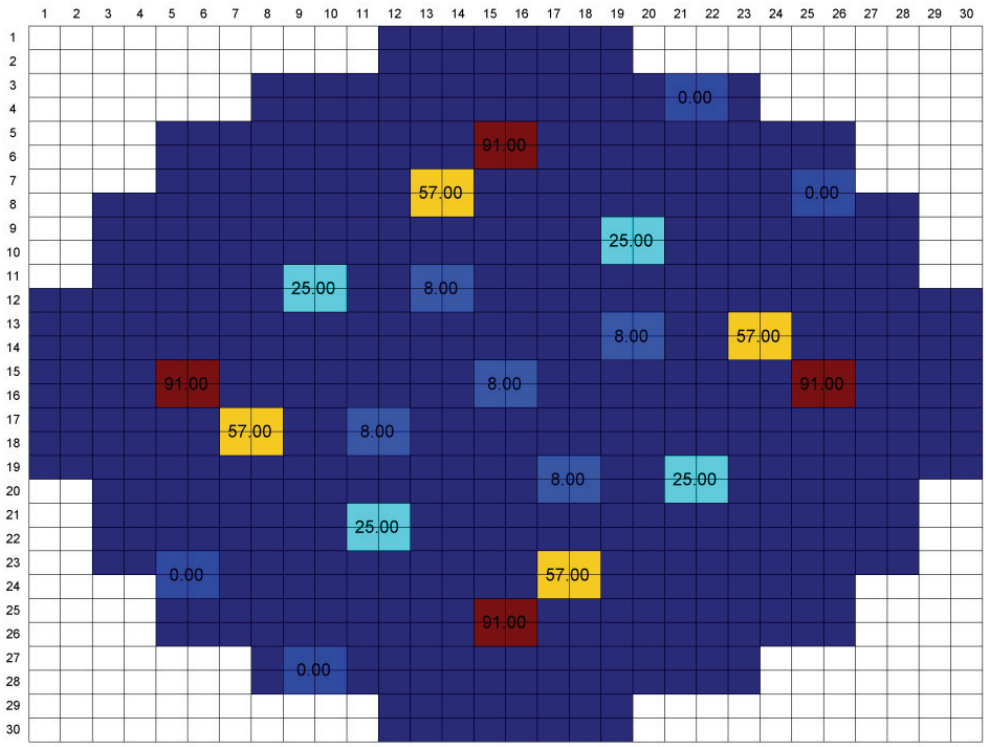

Figure 3-12 Forsmark-2 BWR unit, fuel cycle 21, exposure 2.311 GWd/tHM: control rods that are inserted and their positions in steps withdrawn ('100' is the value for a control rod that is completely withdrawn)

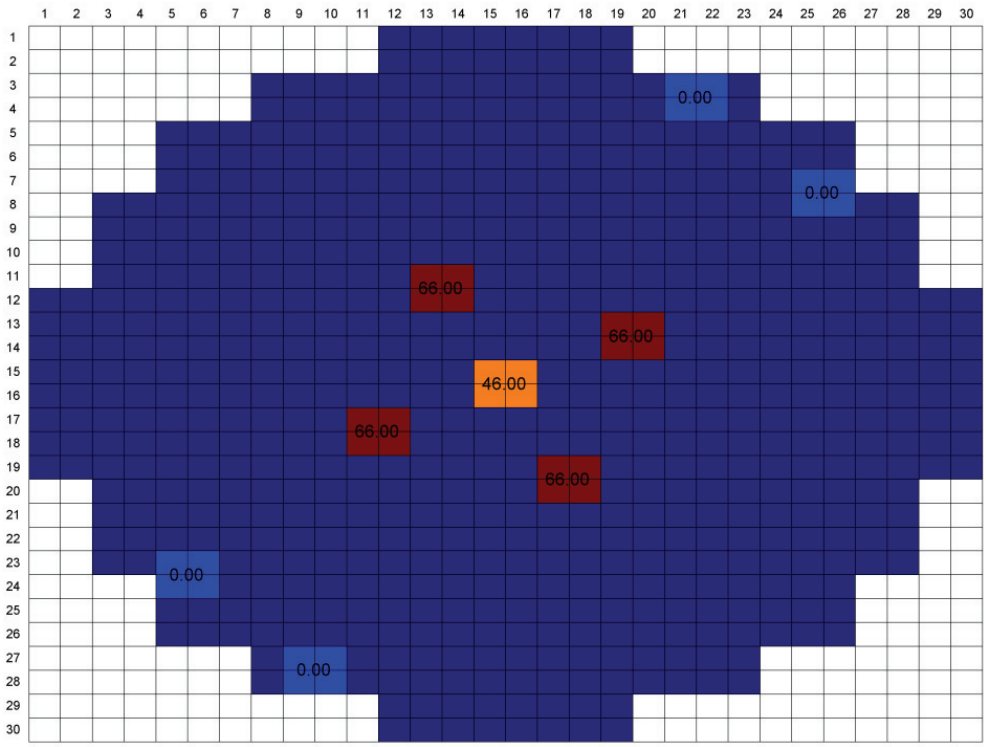

Figure 3-13 Forsmark-2 BWR unit, fuel cycle 21, exposure 5.191 GWd/tHM: control rods that are inserted and their positions in steps withdrawn ('100' is the value for a control rod that is completely withdrawn)

Figures 3-14 to 3-16 show the comparison between the calculated axial power profile and the profile estimated from the detector signals *via* SIMULATE-3, for the beginning, the middle and the end of the cycle, respectively. From these plots, the prediction of the axial power profile is quite satisfactory, throughout the entire fuel cycle. However, it can be noticed that larger discrepancies occur in the lowest axial half of the core (and, indeed, BWR control rods are inserted from the bottom of the core). Since control rods are inserted from the bottom of the core in BWRs, this suggests that the model for the control rods implemented in PARCS might be somehow inaccurate.

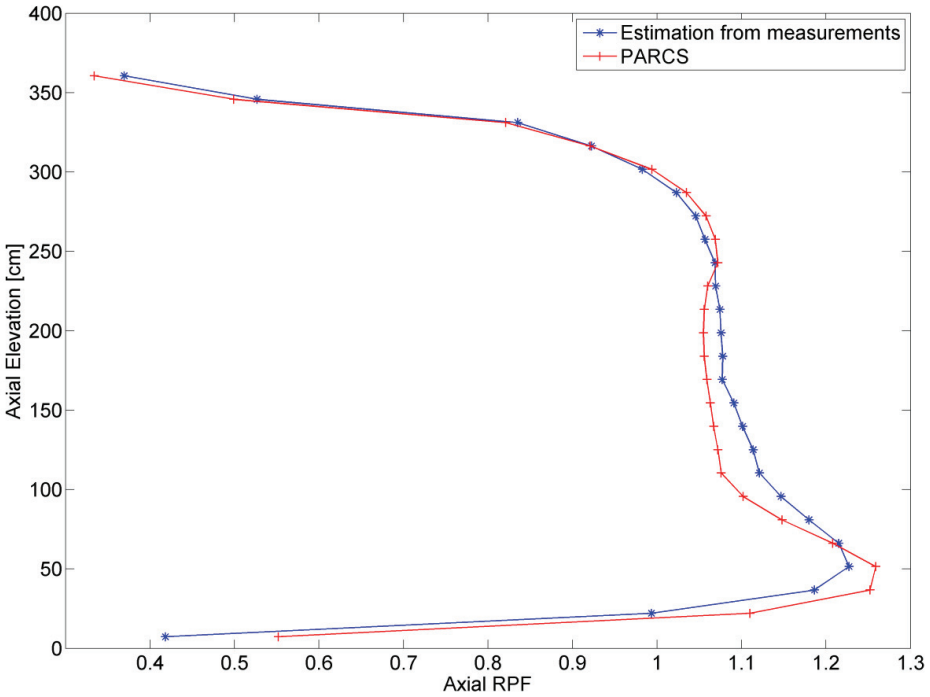

Figure 3-14 Forsmark-2 BWR unit, fuel cycle 21, exposure 0.341 GWd/tHM: axial power profile

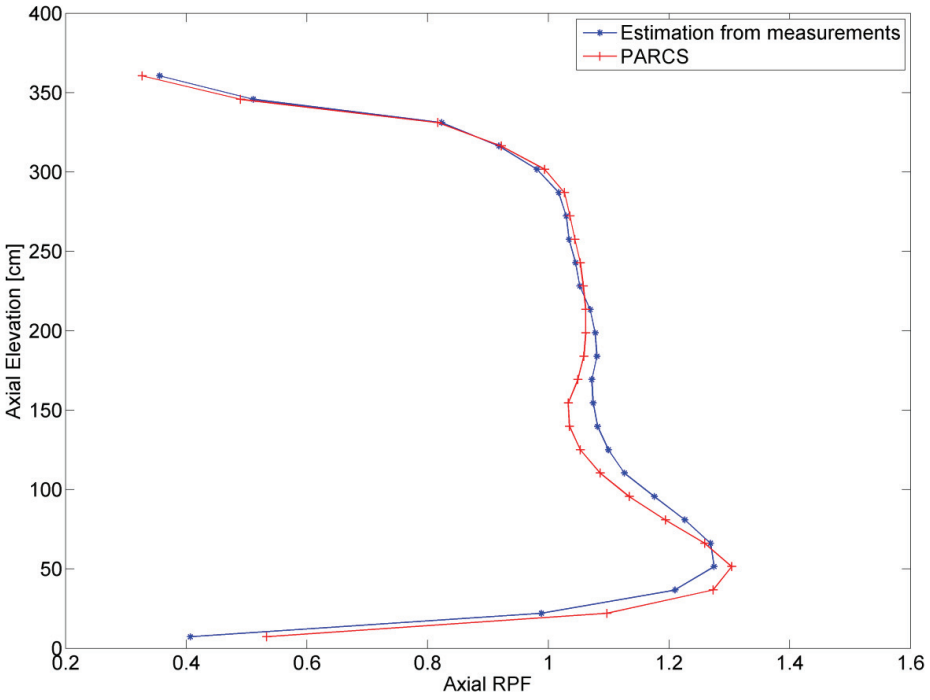

Figure 3-15 Forsmark-2 BWR unit, fuel cycle 21, exposure 5.191 GWd/tHM: axial power profile

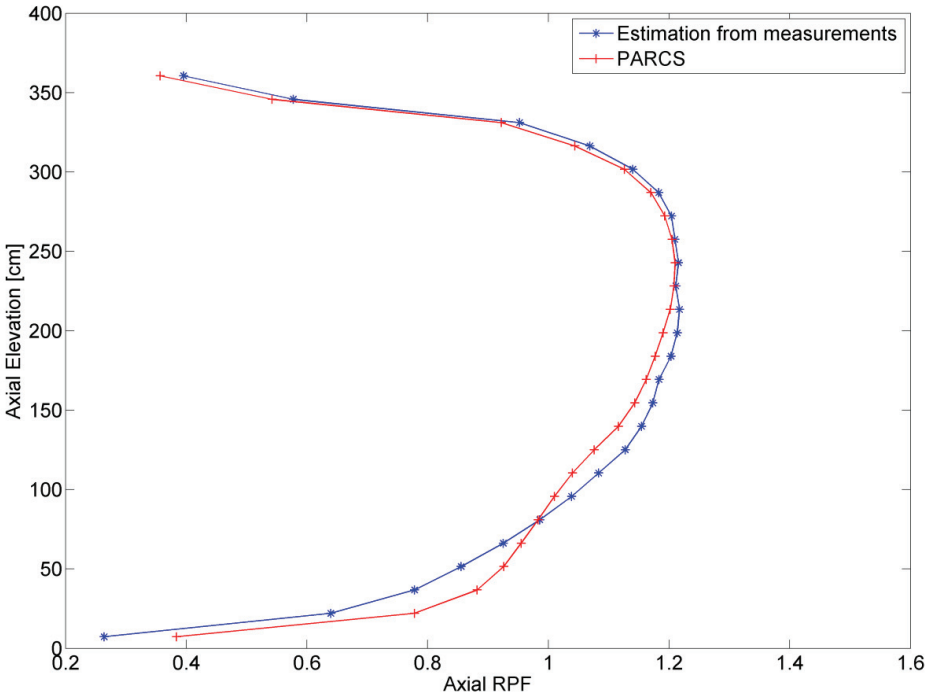

Figure 3-16 Forsmark-2 BWR unit, fuel cycle 21, exposure 5.191 GWd/tHM: axial power profile

Figures 3-17 to 3-18 provide the relative differences (see eq. 3-1), for each fuel assembly, between the calculated RPFs and the RPFs that are derived from the detector signals *via* SIMULATE-3, again, at the beginning, middle, and end of the cycle, respectively. When the radial power distribution is investigated, one can find that the discrepancies are quite significant for those fuel assemblies close to the control rods and less pronounced in the region less affected by the control rods (e.g., see Fig. 3-11 together with Fig. 3-17). Moreover, near the control rods, the RPFs for the majority of the fuel assemblies are underestimated, whereas a relatively strong RPF overestimation is achieved for a few fuel assemblies. This fact seems to point out that a problem in the modeling of control rods exists in. As a matter of fact, an issue with the modeling of multiple composition control rods is known by the PARCS developers, who are currently working on resolving such an issue [15]. Since all control rods in the present Forsmark-2 model are multiple composition control rods, the discrepancies noticed in Figs. 3-17 to 3-19 may thus be attributed to such a pending issue of the PARCS code.

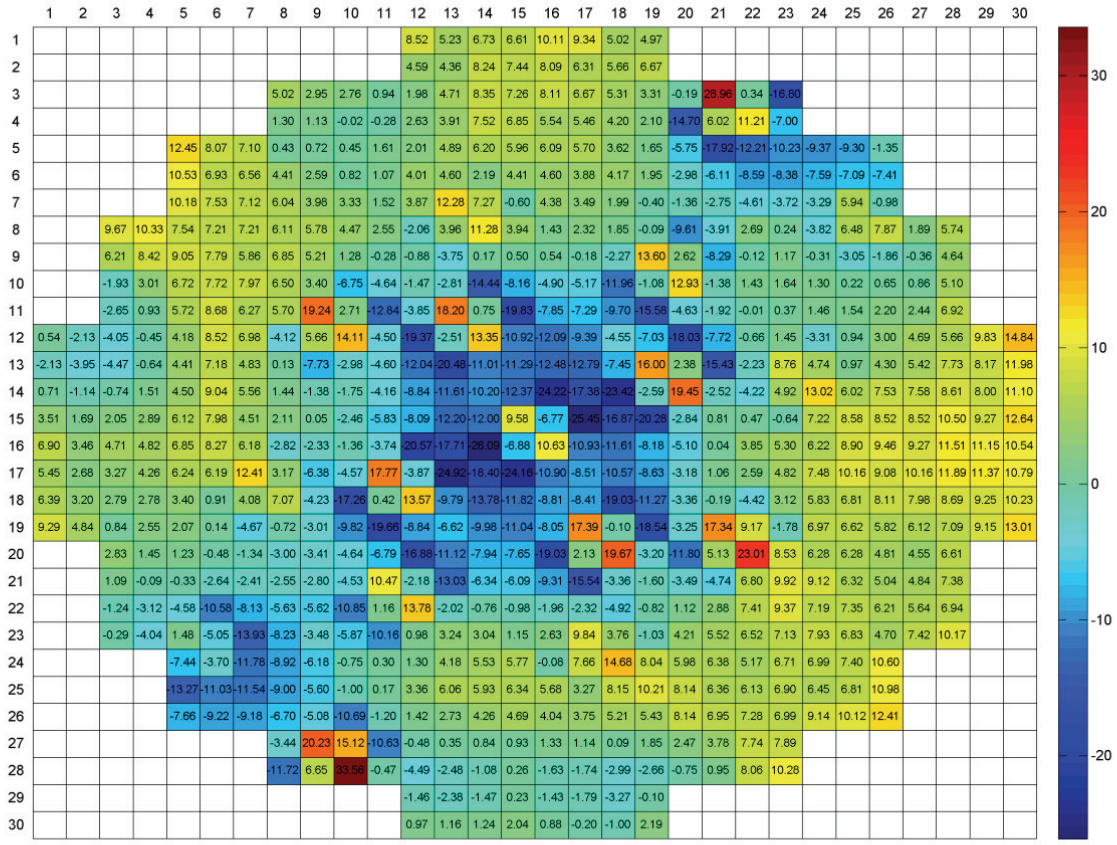

Figure 3-17 Forsmark-2 BWR unit, fuel cycle 21, exposure 0.341 GWd/tHM: radial RPF relative differences (%)

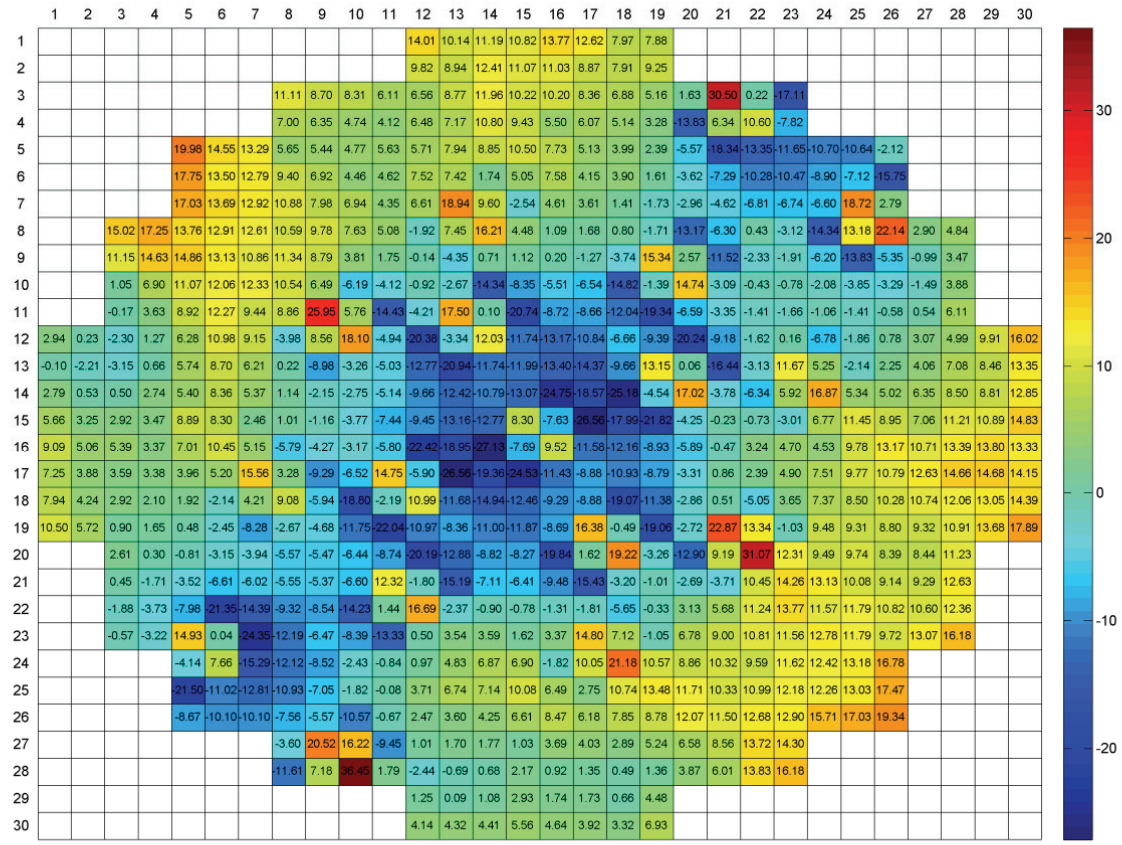

Figure 3-18 Forsmark-2 BWR unit, fuel cycle 21, exposure 2.311 GWd/tHM: radial RPF relative differences (%)

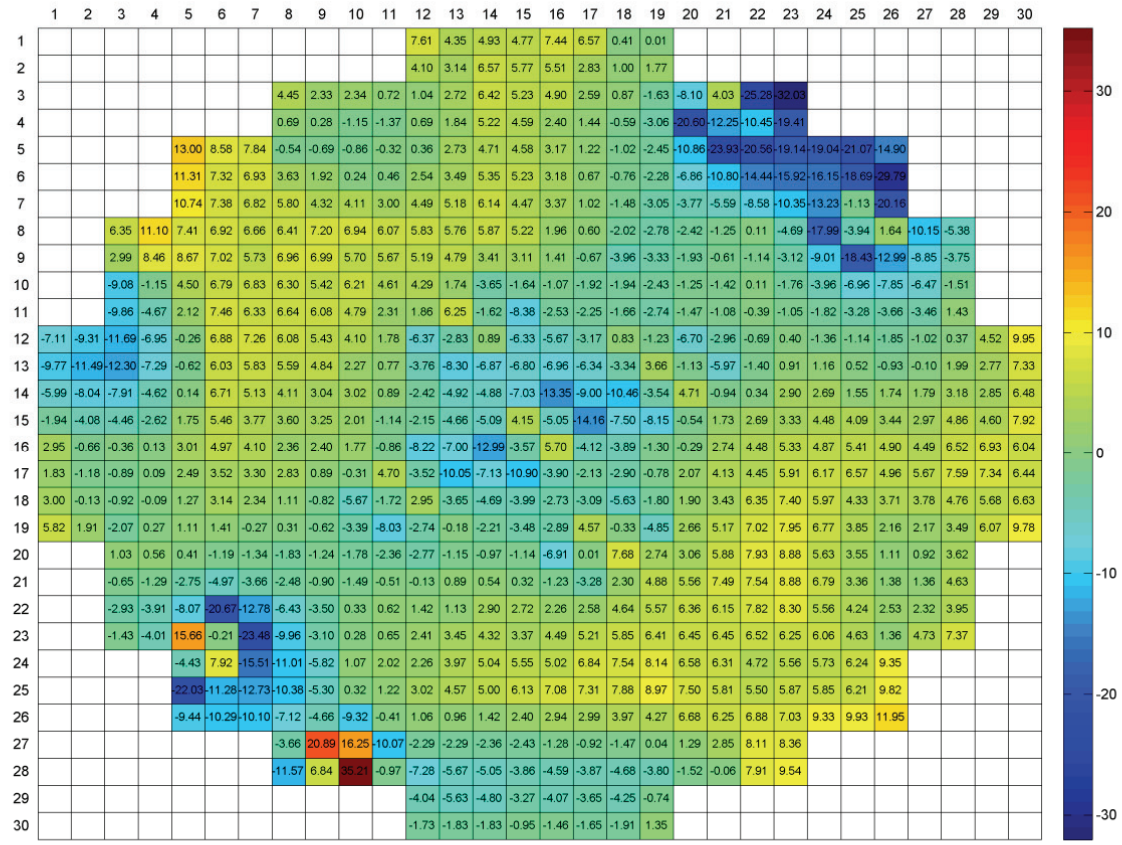

Figure 3-19 Forsmark-2 BWR unit, fuel cycle 21, exposure 5.191 GWd/tHM: radial RPF relative differences (%)

The results obtained for the several sets of TIP measurements performed in Forsmark-2 are summarized in Table 3-4. It can be seen that the total average value of the relative differences between PARCS and measured relative power fraction does not exhibit any strong bias (in fact it is between -0.71% and 2.34%), whereas the minimum and maximum values of the relative differences computed over all the nodes in which the core was discretized underline that the PARCS calculations are not completely satisfactory. Besides, the k_{eff} is predicted relatively well, with a deviation from criticality within +437.1 pcm and -731.8 pcm.

Table 3-4 Forsmark-2 BWR unit, Summary of the assembly-wise deviations in power density

Fuel Cycle	**Exposure** [GWd/tHM]	**Calculated k_{eff}**	**Relative difference between PARCS and measured relative power fraction** (%)		
			Average	Minimum	Maximum
21	0.341	1.004371	0.09	-34.06	61.00
21	2.311	1.001700	1.9	-37.67	65.07
21	5.191	1.003494	0.25	-67.24	75.15
24	0.485	0.996145	-0.71	-39.29	51.10
24	4.622	0.995974	0.93	-34.41	42.26
24	7.394	0.997569	0.5	-36.38	30.54
25	0.135	0.992682	1.69	-29.63	49.88
25	3.050	0.993217	1.23	-35.15	52.07
25	5.731	0.992794	2.34	-38.17	45.17

4. SUMMARY AND CONCLUSIONS

A comparison study has been presented for the U.S. NRC 3-D core neutronics simulator PARCS. In the present report, the work includes an evaluation of the performances of the code for both PWR and BWR applications.

For this purpose, the Swedish Ringhals-3 PWR and the Forsmark-2 BWR cores were modeled with PARCS, and analyzed at about the beginning, the middle, and the end of three different fuel cycles (except for the Ringhals-3 fuel cycle 22, for which the data at the end of cycle were not available). Then, the PARCS simulations were compared against the axial power and the radial power distribution estimated from proper in-core detector measurements.

First of all, no significant difference between the simulations computed with PARCS version 2.71 and 3.0 was observed for both the PWR and the BWR cases (see Figs. 3-1 and 3-2, and Figs 3-9 and 3-10).

As regards the PWR case, the predictions achieved with PARCS reproduce the main variations of the radial and axial power distributions over the core, and show a good agreement in the range of a few percents (see, for instance, Figs. 3-3 and 3-6, and Table 3-2). However, the PARCS simulation at the beginning of a fuel cycle seems to overestimate the power in the center of the core, and to underestimate the power at the periphery, whereas, at the end of a fuel cycle, the situation is the opposite.

Concerning the BWR application, it was found that the PARCS results can capture quite well the behavior of the axial core power, although quite significant discrepancies can be observed in the radial power distribution (see, for instance, Figs. 3-14 and 3-17, and Table 3-4). The reason behind this shortcoming seems to be due to the fact that the control rod model implemented in PARCS is not fully adequate for describing multiple composition control rods as is the case for BWRs (e.g., see Fig. 3-11 together with Fig. 3-17). In this regard, the PARCS team has announced that work has already started to resolve such an issue [15].

For the effective multiplication factor k_{eff}, calculations give reasonable values with respect to the critical value: within ± 200 pcm for most of the PWR cases, and between +437.1 pcm and -731.8 pcm for the BWR cases (again, see Tables 3-2 and 3-4).

In the framework of this study, an alternative interface was also developed and verified successfully for both PWR and BWR applications (see Fig. 2-3), and allows creating the PMAXS files (that are needed for PARCS to generate the cross-sections and the neutron kinetic parameters with respect to the nodal reactor core conditions) directly from the SIMULATE-3 output and library files. No CASMO-4 input file is necessary to create the PMAXS files, as is for instance the case with the GenPMAXS interface. The developed interface thus represents an alternative and complementary procedure to generate cross-sections data to PARCS, in comparison with GenPMAXS.

5. REFERENCES

1. Downar, T.J., Barber, D.A., Miller, R.M., et al., PARCS: Purdue advanced reactor core simulator, in: Proceeding of the International Meeting on New Frontiers of Nuclear Technology: Reactor Physics, Safety and High-Performance Computing (PHYSOR 2002), Seoul, South-Korea, October 10-13, 2002.

2. Downar, T., Lee, D., Xu, Y, Kozlowski, T., PARCS v2.6 - U.S. NRC Core Neutronics Simulator – Theory Manual (Draft), School of Nuclear Engineering, Purdue University, W. Lafayette, IN, USA, 2004.

3. Downar, T., Xu, Y., Seker, V., Carlson, D., 2008. PARCS v2.7, U.S. NRC Core Neutronics Simulator, User Manual, 2008.

4. Stålek, M., Bánáti, J., Demazière, C., Main Steam Line Break Calculations using a coupled RELAP5/PARCS model for the Ringhals-3 Pressurized Water Reactor, in: Proceeding of ICONE 16, Orlando, Florida, USA, May 11-15, 2008.

5. Casal, J.J., Stamm'ler, R.J.J., Villarino, E.A., et al., HELIOS: Geometric capabilities of a new fuel-assembly program, in: Proceedings of the International Topical Meeting in Advances in Mathematics, Computations and Reactor Physics, Pittsburgh, PA, USA, April 28 – May 2, 1991, Vol. 2, 10.21-1.

6. Ekberg, K., Forssén, B.-H., Knott, D., Umbarger, J.A., Edenius, M., CASMO-4: A fuel assembly burnup program, User's Manual, Studsvik Scandpower, Studsvik/SOA-95/10S, 1995.

7. Xu, Y., Downar, T., GenPMAXS Code for Generating the PARCS Cross Section Interface File PMAXS, Purdue University, School of Nuclear Engineering, West Lafayette, IN, USA, 2006.

8. Covington, L.J., Cronin, J.T., Umbarger, J.A., SIMULATE-3: Advanced three-dimensional two-group reactor analysis code, Studsvik Scandpower, Studsvik/SOA-95/15 Rev 2, 1995.

9. Stålek, M., Demazière, C., Development and validation of a cross-section interface for PARCS, Annals of Nuclear Energy 35, 2008.

10. Ver Planck, D.M., Smith, K.S., Umbarger, J.A., TABLES-3 users's manual, Studsvik Scandpower/SOA-95/16, 1995.

11. Garis, N.S., PWR model with CASMO and SIMULATE, Studsvik Scandpower, Studsvik/SOA-95/10S, 1995.

12. Garis, N.S., BWR model with CASMO and SIMULATE, Studsvik Scandpower, Studsvik/SOA-95/11S, 1995.

13. Vanevenhoven, S., private communication, Studsvik Scandpower, Idaho Falls, ID, USA, 2005.

14. Xu, Y., Private communication, Purdue University, School of Nuclear Engineering, West Lafayette, IN, USA, 2005.

15. Hudson, N., Downar, T., XU, Y., PARCS Status, presentation at the: Spring CAMP Meeting, Bariloche, Rio Negro, Argentina, April 27-29, 2011.

NRC FORM 335
(9-2004)
NRCMD 3.7

U.S. NUCLEAR REGULATORY COMMISSION

1. REPORT NUMBER
(Assigned by NRC, Add Vol., Supp., Rev., and Addendum Numbers, if any.)

NUREG/IA-0414

BIBLIOGRAPHIC DATA SHEET

(See instructions on the reverse)

2. TITLE AND SUBTITLE

Comparison of the U.S. NRC PARCS Core Neutronics Simulator Against In-Core Detector Measurements for LWRs Applications

3. DATE REPORT PUBLISHED

MONTH	YEAR
April	2012

4. FIN OR GRANT NUMBER

5. AUTHOR(S)

C. Demazière, M. Stålek, P. Vinai

6. TYPE OF REPORT

Technical

7. PERIOD COVERED *(Inclusive Dates)*

8. PERFORMING ORGANIZATION - NAME AND ADDRESS *(If NRC, provide Division, Office or Region, U.S. Nuclear Regulatory Commission, and mailing address; if contractor, provide name and mailing address.)*

Division of Nuclear Engineering
Chalmers University of Technology
SE-41296 Gothenburg
Sweden

9. SPONSORING ORGANIZATION - NAME AND ADDRESS *(If NRC, type "Same as above"; if contractor, provide NRC Division, Office or Region, U.S. Nuclear Regulatory Commission, and mailing address.)*

Division of Systems Analysis
Office of Nuclear Regulatory Research
U.S. Nuclear Regulatory Commission
Washington, DC 20555-0001

10. SUPPLEMENTARY NOTES

A. Calvo, NRC Project Manager

11. ABSTRACT *(200 words or less)*

The safety analysis of a Nuclear Power Plant (NPP) is based on the application of complex computer codes that are able to simulate the physical behaviour of the system under normal operations and abnormal conditions. Therefore, such codes must be extensively and continuously verified and validated in order to demonstrate their reliability. In this light, the current document presents an assessment study for the U.S. NRC 3-D neutronic core simulator PARCS, and it includes an evaluation of the performances of the code against in-core neutron flux measurements taken at the Swedish Ringhals-3 Pressurized Water Reactor (PWR) unit and at the Swedish Forsmark-2 Boiling Water Reactor (BWR) unit. In the PWR case, the PARCS simulations predict satisfactorily both the core axial power profile and the core radial power distribution, although some deviations of the results from the measurements were observed and need to be further investigated. In the BWR case, quite significant discrepancies between the calculated and the measured power distribution over the core were found. The reported investigations suggest that the control rod model implemented in PARCS might not be fully adequate.

This work has been performed with financial support from the Swedish Radiation Safety Authority (SSM).

12. KEY WORDS/DESCRIPTORS *(List words or phrases that will assist researchers in locating the report.)*

PARCS
Swedish Ringhals-3 Pressurized Water Reactor (PWR)
Swedish Forsmark-2 Boiling Water Reactor (BWR)
Swedish Radiation Safety Authority (SSM)
Chalmers University of Technology
SIMULATE-3
NRC 3-D neutronic core simulator

13. AVAILABILITY STATEMENT

unlimited

14. SECURITY CLASSIFICATION

(This Page)
unclassified

(This Report)
unclassified

15. NUMBER OF PAGES

16. PRICE

Federal Recycling Program

UNITED STATES
NUCLEAR REGULATORY COMMISSION
WASHINGTON, DC 20555-0001

OFFICIAL BUSINESS

NUREG/IA-0414

Comparison of the U.S. NRC PARCS Core Neutronics Simulator Against In-Core Detector Measurements for LWR Applications

April 2012